Available online at www.sciencedirect.com
SCIENCE DIRECT
ELSEVIER
Biochemical and Biophysical Research Communications 347 (2006) 261–265
BBRC
www.elsevier.com/locate/ybbrc

Mechanisms of establishment of persistent SARS-CoV-infected cells

Tetsuya Mizutani [a,*], Shuetsu Fukushi [a], Koji Ishii [b], Yuko Sasaki [c], Tsuyoshi Kenri [c], Masayuki Saijo [a], Yumi Kanaji [d], Kinji Shirota [d], Ichiro Kurane [a], Shigeru Morikawa [a]

[a] *Department of Virology 1, National Institute of Infectious Diseases, Gakuen 4-7-1, Musashimurayama, Tokyo 208-0011, Japan*
[b] *Department of Virology 2, National Institute of Infectious Diseases, 1-23-1 Toyama, Shinjuku-ku, Tokyo 162-8640, Japan*
[c] *Department of Bacteriology 2, National Institute of Infectious Diseases, Gakuen 4-7-1, Musashimurayama, Tokyo 208-0011, Japan*
[d] *Research Institute of Biosciences, Azabu University, 1-71-1 Futinobe, Sagamihara-shi, Kanagawa 229- 8501, Japan*

Received 6 June 2006
Available online 22 June 2006

Abstract

Previously, we reported the establishment of cells with persistent SARS-CoV infection after apoptotic events and showed that both JNK and PI3K/Akt signaling pathways are important for persistence by treatment with inhibitors at the early stages of SARS-CoV infection. However, the mechanisms of establishment of persistent infection are still unclear. In this study, we investigated which signaling pathways play important roles in escape from apoptosis in cells infected with SARS-CoV. In persistently infected cells at 50 h.p.i., PI3K/Akt, JNK, p38 MAPK and Bcl-2 were phosphorylated and the protein levels of Bcl-2 and Bcl-xL were increased. When surviving cells were treated with the JNK-specific inhibitor, SP600125, at 50 h.p.i., all cells died, suggesting that the JNK signaling pathway is necessary for maintenance of persistently infected cells. Among the signaling pathways in persistently infected cells, Akt and JNK were phosphorylated in SARS-CoV-nucleocapsid (N) protein-expressing Vero E6 cells using vaccinia viral vector (DIs), strongly suggesting that N protein-induced phosphorylation of Akt and JNK are necessary to establish persistence. These results indicated that at least four proteins, Akt, JNK, Bcl-2 and Bcl-xL, are necessary for survival of persistently SARS-CoV-infected cells.

Keywords: SARS; JNK; Bcl-2; Bcl-xL; Nucleocapsid protein

Severe acute respiratory syndrome (SARS) is a newly discovered infectious disease with atypical pneumonia caused by SARS coronavirus (SARS-CoV). SARS became a global health threat due to its rapid transmission and high fatality rate [1,2].

Vero E6 is a cell line derived from African green monkey kidney cells and is sensitive to SARS-CoV. Many laboratories use this cell line to study SARS-CoV. Infection of Vero E6 cells with SARS-CoV induces apoptosis *via* activation of caspase-3 [3]. Akt and mitogen-activated protein kinases (MAPKs), including c-Jun N-terminal protein kinase (JNK), extracellular signal-related kinase (ERK) 1/2, and p38 MAPK, are phosphorylated in SARS-CoV-infected Vero E6 cells [3–5]. Especially, activation of p38 and inactivation of Akt by SARS-CoV infection induce cytopathic effects and apoptosis in virus-infected cells, respectively. Phosphorylation of p38 MAPK is known to regulate signal transducer and activator of transcription 3 and 90 kDa ribosomal S6 kinases [5,6]. Although the majority of virus-infected cells die by apoptosis, we found that a small population of virus-infected cells remained alive and these cells grew with production of virus [7]. Four groups, including ours, independently reported persistent infection of cultured cells by SARS-CoV [8–10]. We found that JNK and PI3K/Akt signaling pathways are important for the establishment of persistent SARS-CoV infection in Vero E6 cells when these specific inhibitors were added soon after viral adsorption.

In this study, we further analyzed the mechanisms of establishment of persistent SARS-CoV infection in Vero

* Corresponding author. Fax: +81 42 564 4881.
E-mail address: tmizutan@nih.go.jp (T. Mizutani).

0006-291X/$ - see front matter © 2006 Elsevier Inc. All rights reserved.
doi:10.1016/j.bbrc.2006.06.086

E6 cells. We found that anti-apoptotic proteins, Bcl-2 and Bcl-xL, are important for persistent infection. Nucleocapsid (N) protein of SARS-CoV was suggested to play important roles in phosphorylation of Akt and JNK.

Materials and methods

Cells and virus. Vero E6 cells were subcultured routinely in 75-cm^3 flasks in Dulbecco's modified Eagle's medium (DMEM; Sigma, St. Louis, MO, USA) supplemented with 0.2 mM L-glutamine, 100 U/ml penicillin, 100 μg/ml streptomycin, and 5% (v/v) fetal bovine serum (FBS), and maintained at 37 °C in an atmosphere of 5% CO_2. The medium was changed to 2% FBS DMEM before virus infection. SARS-CoV, which was isolated as Frankfurt 1 and kindly provided by Dr. J. Ziebuhr, was used in the present study. Infection was usually performed at a multiplicity of infection (m.o.i.) of 5. DIs-N expressing N RNA of SARS-CoV and DIs-GFP expressing GFP RNA were described in our previous study [11]. Confluent Vero E6 cells were infected with DIs-N and -GFP at 5 m.o.i.

Fixing and staining of cells. The cells in 24-well plates were fixed with 10% formaldehyde for at least 24 h, and stained with 0.1% naphthol blue-black for 30 min. This convenient method was described by Everitt and Wohlfart for determination of the actual or relative number of cells in anchorage culture [12]. After washing out with water, the plates were scanned with a GT-9400UF scanner (Epson, Tokyo, Japan). The dye–protein complexes were released hydrolytically with 0.1 M NaOH and measured spectrophotometrically at 660 nm. When cells and the supernatant contained infectious SARS-CoV, the cell number was counted using this method. The number of cells that did not contain SARS-CoV was counted using the WST-1 cell proliferation assay system (Takara, Shiga, Japan).

Inhibitors. The JNK inhibitor, SP600125, and PI3K/Akt inhibitor, LY294002, were purchased from Calbiochem (San Diego, CA, USA) and Cell Signaling Technology Inc. (Beverly, MA, USA), respectively. These inhibitors were dissolved in dimethyl sulfoxide (DMSO) at a concentration of 10 mM. The same volume of DMSO alone was used as a control.

Western blotting. The whole-cell extracts were electrophoresed on 5–20% gradient polyacrylamide gels, and transferred electrophoretically onto PVDF membranes (Immobilon-P; Millipore, Bedford, MA, USA). In the present study, we applied two sets of samples to polyacrylamide gels, and the membranes were divided into two halves after blotting, or membranes were examined once using a LumiGLO Elite chemiluminescent system (Kirkegaard and Perry Laboratories, Gaithersburg, ML, USA), and then stripped using Restore Western blot stripping buffer (Pierce, Rockford, IL, USA) for the second detection. The following antibodies, obtained from Cell Signaling Technology Inc., were used in the present study at a dilution of 1:1000: rabbit anti-phospho Akt (Ser473) antibody, rabbit anti-Akt antibody, rabbit anti-phospho ERK (Thr202/Tyr204) antibody, rabbit anti-ERK antibody, rabbit anti-p38 MAPK (Thr180/Tyr182) antibody, rabbit anti-p38 MAPK antibody, rabbit anti-phospho SAPK/JNK (Thr183/Tyr185) antibody, rabbit anti-SAPK/JNK antibody, rabbit anti-phospho Bcl-2 (Ser 70) antibody, and anti-Bcl-xL antibody. Mouse anti-Bcl-2 antibody was purchased from BD Biosciences (Franklin Lakes, NJ, USA) and used at a dilution of 1:500. Mouse anti-β-actin antibody was purchased from Sigma and used at a dilution of 1:5000. Rabbit anti-SARS Nucleocapsid protein antibody was described previously [3].

Results

Phosphorylation of signaling pathways in cells persistently infected by SARS-CoV

As indicated in our previous studies, apoptotic signals, cleaved caspase-3 and DNA fragmentation, are detected at 18 and 24 h post-infection (h.p.i.) in SARS-CoV-infected Vero E6 cells [3]. At 24 h.p.i., cells begin to show rounding and persistently infected cells are observed after 48 h.p.i. To investigate which signaling pathways are phosphorylated in persistently SARS-CoV-infected cells, protein samples were obtained from these cells at 50 h.p.i. Vero E6 cells were prepared at confluency in T-25 flasks with 2% fetal bovine serum (FBS) containing Dulbecco's modified Eagle's medium (DMEM), and infected with SARS-CoV at 5 m.o.i. On the other hand, Vero E6 cells were prepared in T-25 flasks at several concentrations with 2% FBS containing DMEM as controls because surviving cell number is different (less than 5% of total cells) in each experiment. At 50 h.p.i., surviving cells and controls were washed with 2% FBS containing DMEM 5 times (with pipetting 25 times). Although most dead cells were washed out, a fraction of dead cells were attached to surviving cells and could not be removed completely by washing. As phosphorylation status of signaling pathways sometimes changes following trypsinization and centrifugation, sample buffer for Western blotting analysis was added directly to the washed cells. We obtained a protein sample from mock-infected cells, with a similar cell number to persistently infected cells. The protein samples seemed to contain a maximum of 50% proteins from surviving cells. Western blotting analysis was performed using antibodies to phosphorylated proteins of signaling pathways. As shown in Fig. 1, Akt, JNK, and p38 MAPK were phosphorylated in surviving cells. On the other hand, Akt was phosphorylated in control cells, while JNK and p38 MAPK were not. As Akt was dephosphorylated in both confluent and subconfluent cells after 18 h.p.i. as shown in our previous studies [4,13], detection of strongly phosphorylated Akt was

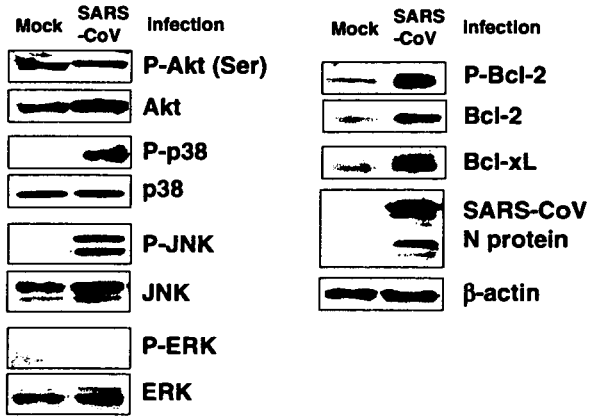

Fig. 1. Phosphorylation status of signaling pathways in persistently SARS-CoV-infected cells. Vero E6 cells were prepared at confluency in T-25 flasks with 2% fetal bovine serum (FBS) containing Dulbecco's modified Eagle's medium (DMEM), and infected with SARS-CoV at 5 m.o.i. At 50 h.p.i., surviving cells and controls were washed 5 times with 2% FCS containing DMEM (pipetting a total of 25 times). Mock-infected subconfluent cells, similar in number to surviving cells that had escaped from apoptosis by SARS-CoV infection, were also washed in the same manner. Western blotting analysis was performed using these protein samples.

suggested to reflect a feature of surviving cells that had escaped from cell death. In addition, the phosphorylated Akt in surviving cells indicated anti-apoptotic activity. The levels of the anti-apoptotic proteins, Bcl-2 and Bcl-xL, and phosphorylated Bcl-2, were also increased in surviving cells. The anti-apoptotic Bcl-2 family proteins, Bcl-2 and Bcl-xL, play important roles in inhibiting mitochondria-dependent cell death pathways [14]. This result suggested that Akt and JNK are important to establish persistent infection as indicated in our previous study, and that Bcl-xL and Bcl-2 are important for survival. Interestingly, p38 MAPK was strongly phosphorylated in surviving cells, suggesting that persistently infected cells consist of a balance between cell death and survival.

Importance of PI3K/Akt and JNK for establishment of persistently virus-infected cells

In our previous study, we showed that treatment of Vero E6 cells with the JNK inhibitor, SP600125, and PI3K/Akt inhibitor, LY294002, 1 h after inoculation with SARS-CoV prevented persistent SARS-CoV infection [7]. Therefore, we concluded that activation of JNK and PI3K/Akt by SARS-CoV infection is important for the establishment of persistence. To investigate whether these inhibitors affect the establishment of viral persistence in cells at the late stage of SARS-CoV infection, cells were treated with inhibitors at 50 h.p.i. As shown in Fig. 2A and B, SP600125 killed the cells completely, while LY294002 did not. As LY294002 has an inhibitory effect on cell proliferation, as indicated in Fig. 2C and in our previous study [13], the growth rate of persistently infected cells was slow. On the other hand, treatment with SP600125 in the absence of SARS-CoV infection did not affect cell proliferation. As Akt in virus-infected cells was dephosphorylated after 18 h.p.i., as shown in our previous studies [4,13], phosphorylation of Akt at the early stage of infection may be important for preventing apoptosis. However, this result strongly suggested that once persistence is established, phosphorylation of Akt is not necessary for survival. Therefore, we concluded that activation of PI3K/Akt is essential for the establishment of persistent infection with SARS-CoV at time points before cell death, whereas activation of JNK is required at the time of establishment of persistence.

Phosphorylation of signaling pathways by SARS-CoV-nucleocapsid protein

Next, we investigated which signaling pathways are phosphorylated by nucleocapsid (N) protein of SARS-CoV because several reports indicated that expression of N protein induces phosphorylation of signaling pathways. Surjit et al. reported that ERK, phosphorylated Akt and Bcl-2 are down-regulated, whereas JNK, p38 MAPK activation, activated caspase-3 and -7 are up-regulated in COS-1 cells in the absence of growth factors [15]. They

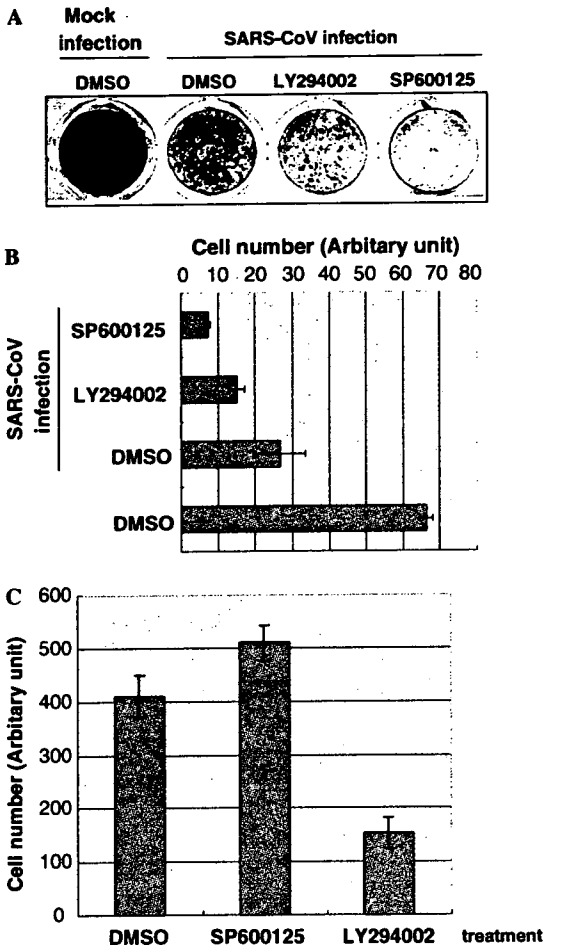

Fig. 2. Effects of JNK and PI3K/Akt inhibitors on cell viability of persistently SARS-CoV-infected cells. (A) Confluent Vero E6 cells in 24-well plates were infected with SARS-CoV for 50 h, and then LY294002 (10 μM) and SP600125 (20 μM) were added to the cells. All wells contained the same volume of DMSO. After incubation for 7 days, the cells were fixed with 10% formaldehyde and stained with 0.1% naphthol blue-black. (B) Stained cells were quantified by measuring the absorbance at OD_{660} with addition of NaOH. (C) Subconfluent cells were treated with inhibitors for 5 days, and then cells were counted using the WST-1 cell proliferation assay system [6].

suggested that N protein is able to induce apoptosis under stress conditions. To understand which signaling pathways are phosphorylated by N protein in Vero E6 cells persistently infected with SARS-CoV, we made an N expression plasmid. Transfection of the N expression plasmid was performed using transfection reagents, Magnetfection and VeroFect (OZ Biosciences, Marseille, France), which our screen of transfection reagents suggested to be the best transfection systems for Vero E6 cells, which have low transfection efficiency (data not shown). However, levels of expression of N protein by these two reagents were far lower than those in SARS-CoV-infected Vero E6 cells. Therefore, we next used the vaccinia virus expression system (DIs-N) [11]. Vero E6 cells were infected with DIs-N at 5 m.o.i. and protein samples were obtained at 18 h.p.i.

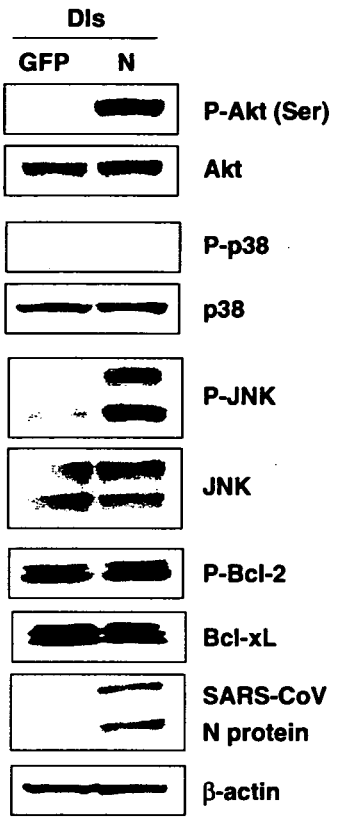

Fig. 3. Modulation of signaling pathways by N expression. Confluent Vero E6 cells in 24-well plates were infected with DIs-N and DIs-GFP at 5 m.o.i. Protein samples were obtained at 18 h.p.i. and Western blotting analysis was performed.

We used DIs-GFP, which expresses GFP protein in infected cells, as a control at the same m.o.i. As shown in Fig. 3, both Akt and JNK were phosphorylated in DIs-N-infected cells as compared with DIs-GFP-infected cells. There was no significant difference in the amount of Bcl-2, Bcl-xL, and phosphorylated p38 MAPK. This result suggested that phosphorylation of Akt and JNK induced by N protein in SARS-CoV-infected Vero E6 cells plays important roles for the establishment of persistence.

Discussion

In our previous study, the signaling pathways of JNK and Akt were shown to be important for establishment of persistent SARS-CoV infection, when these inhibitors were added soon after SARS-CoV infection [7]. Approximately 95% of confluent Vero E6 cells died 2 days after infection with SARS-CoV. The remaining 5% of cells that survived grew with persistent virus infection. When 24-well plates were used for experiments, the persistently infected cells reached confluence by 7 days. Interestingly, the PI3K/Akt inhibitor, LY294002, permitted cell survival when added after apoptotic events, but activation of JNK was also necessary for survival after apoptotic events. Our previous study demonstrated the importance of Akt activation for proliferation of SARS-CoV-infected cells [4]. Phosphorylation of Akt was down-regulated in subconfluent cells by SARS-CoV infection [13]. Nevertheless, LY294002-treated surviving cells that had escaped from SARS-CoV-induced apoptosis could still grow slowly. One of the reasons for this is that PI3K/Akt inhibitor needs 3 days after treatment to inhibit cell proliferation [13]. Therefore, persistent cell colonies may grow slightly in the presence of LY294002. SARS-CoV replicates in surviving cells, and these cells are still alive in the presence of LY294002, suggesting that the signaling pathway of PI3K/Akt is not necessary to prevent apoptosis in cells with persistent virus infection. The apoptotic signaling pathways may be blocked independent of PI3K/Akt in surviving cells. In this study, we demonstrated that the anti-apoptotic proteins Bcl-2 and Bcl-xL were present at elevated levels in persistently infected cells. Because Bcl-2 is slightly increased and phosphorylated at acute infection (24 h.p.i.), but not Bcl-xL (data not shown), Bcl-xL may be more important than Bcl-2 for survival. These results indicated that the PI3K/Akt signaling pathway is important for cell survival in the early stages of SARS-CoV-induced apoptosis, whereas the JNK, Bcl-2, and Bcl-xL pathways are important after apoptotic events. We found SP600125 that slightly prevented SARS-CoV-induced apoptosis (unpublished data). The JNK signaling pathway is one of the key factors for understanding persistence of SARS-CoV.

Interestingly, when we used the N expression system of vaccinia virus (DIs-N), Akt and JNK were phosphorylated in Vero E6. The differences in the results between our study and that reported by Surjit et al. using COS-1 are most likely due to the use of different cell cultures and different expression systems [15]. It is not yet clear whether N protein alone is able to induce phosphorylation of these signaling pathways in Vero E6 cells because we have no useful system for plasmid transfection of these cells. Both Akt and JNK were phosphorylated in our system due to additional stress by expression of vaccinia viral proteins. Because Bcl-2 and Bcl-xL were not increased by N protein expression, these anti-apoptotic proteins may not be downstream of Akt and JNK signaling pathways.

In this paper, we showed possible mechanisms of establishment of persistent SARS-CoV infection. Further investigations are necessary to determine signaling pathways, which are able to up-regulate Bcl-2 and Bcl-xL levels.

Acknowledgments

We thank Drs. S. Harada (National Institute of Infectious Diseases, Japan) and M. Funaba (Azabu University, Japan) for helpful suggestions. We also thank Ms. M. Ogata (National Institute of Infectious Diseases, Japan) for her assistance. This work was supported in part by the Japan Health Science Foundation and, Japan Society for the Promotion of Science, Tokyo, Japan.

References

[1] M.A. Marra, S.J. Jones, C.R. Astell, R.A. Holt, A. Brooks-Wilson, Y.S. Butterfield, J. Khattra, J.K. Asano, S.A. Barber, S.Y. Chan, A. Cloutier, S.M. Coughlin, D. Freeman, N. Girn, O.L. Griffith, S.R. Leach, M. Mayo, H. McDonald, S.B. Montgomery, P.K. Pandoh, A.S. Petrescu, A.G. Robertson, J.E. Schein, A. Siddiqui, D.E. Smailus, J.M. Stott, G.S. Yang, F. Plummer, A. Andonov, H. Artsob, N. Bastien, K. Bernard, T.F. Booth, D. Bowness, M. Czub, M. Drebot, L. Fernando, R. Flick, M. Garbutt, M. Gray, A. Grolla, S. Jones, H. Feldmann, A. Meyers, A. Kabani, Y. Li, S. Normand, U. Stroher, G.A. Tipples, S. Tyler, R. Vogrig, D. Ward, B. Watson, R.C. Brunham, M. Krajden, M. Petric, D.M. Skowronski, C. Upton, R.L. Roper, The genome sequence of the SARS-associated coronavirus, Science 300 (2003) 1399–1404.

[2] P.A. Rota, M.S. Oberste, S.S. Monroe, W.A. Nix, R. Campagnoli, J.P. Icenogle, S. Penaranda, B. Bankamp, K. Maher, M.H. Chen, S. Tong, A. Tamin, L. Lowe, M. Frace, J.L. DeRisi, Q. Chen, D. Wang, D.D. Erdman, T.C. Peret, C. Burns, T.G. Ksiazek, P.E. Rollin, A. Sanchez, S. Liffick, B. Holloway, J. Limor, K. McCaustland, M. Olsen-Rasmussen, R. Fouchier, S. Gunther, A.D. Osterhaus, C. Drosten, M.A. Pallansch, L.J. Anderson, W.J. Bellini, Characterization of a novel coronavirus associated with severe acute respiratory syndrome, Science 300 (2003) 1394–1399.

[3] T. Mizutani, S. Fukushi, M. Saijo, I. Kurane, S. Morikawa, Phosphorylation of p38 MAPK and its downstream targets in SARS coronavirus-infected cells, Biochem. Biophys. Res. Commun. 319 (2004) 1228–1234.

[4] T. Mizutani, S. Fukushi, M. Saijo, I. Kurane, S. Morikawa, Importance of Akt signaling pathway for apoptosis in SARS-CoV-infected Vero E6 cells, Virology 327 (2004) 169–174.

[5] T. Mizutani, S. Fukushi, M. Murakami, T. Hirano, M. Saijo, I. Kurane, S. Morikawa, Tyrosine dephosphorylation of STAT3 in SARS coronavirus-infected Vero E6 cells, FEBS Lett. 577 (2004) 187–192.

[6] T. Mizutani, S. Fukushi, M. Saijo, I. Kurane, S. Morikawa, Regulation of p90RSK phosphorylation by SARS-CoV infection in Vero E6 cells, FEBS Lett. 580 (2006) 1417–1424.

[7] T. Mizutani, S. Fukushi, M. Saijo, I. Kurane, S. Morikawa, JNK and PI3k/Akt signaling pathways are required for establishing persistent SARS-CoV infection in Vero E6 cells, Biochem. Biophys. Acta 1741 (2005) 4–10.

[8] P.K. Chan, K.F. To, A.W. Lo, J.L. Cheung, I. Chu, F.W. Au, J.H. Tong, J.S. Tam, J.J.J. Sung, H.K. Ng, Persistent infection of SARS coronavirus in colonic cells in vitro, J. Med. Virol. 74 (2004) 1–7.

[9] G. Palacios, O. Jabado, N. Renwick, T. Briese, W.I. Lipkin, Severe acute respiratory syndrome coronavirus persistence in Vero cells, Chin. Med. J. (Engl.) 118 (2005) 451–459.

[10] M. Yamate, M. Yamashita, T. Goto, S. Tsuji, Y.G. Li, J. Warachit, M. Yunoki, K. Ikuta, Establishment of Vero E6 cell clones persistently infected with severe acute respiratory syndrome coronavirus, Microbes Infect. 7 (2005) 1530–1540.

[11] K. Ishii, H. Hasegawa, N. Nagata, M. Mizutani, S. Morikawa, T. Suzuki, F. Taguchi, M. Tashiro, T. Takemori, T. Miyamura, Y. Tsunetsugu-Yokota, Induction of protective immunity against severe acute respiratory syndrome coronavirus (SARS-CoV) infection using highly attenuated recombinant vaccinia virus DIs, Virology (in press).

[12] E. Everitt, C. Wohlfart, Spectrophotometric quantitation of anchorage-dependent cell numbers using extraction of naphthol blue-black-stained cellular protein, Anal. Biochem. 162 (1987) 122–129.

[13] T. Mizutani, S. Fukushi, D. Iizuka, O. Inanami, M. Kuwabara, H. Takashima, H. Yanagawa, M. Saijo, I. Kurane, S. Morikawa, Inhibition of cell proliferation by SARS-CoV infection in Vero E6 cells, FEMS Immunol. Med. Microbiol. 46 (2006) 236–243.

[14] R. Kim, Unknotting the roles of Bcl-2 and Bcl-xL in cell death, Biochem. Biophys. Res. Commun. 333 (2005) 336–343.

[15] M. Surjit, B. Liu, S. Jameel, V.T. Chow, S.K. Lal, The SARS coronavirus nucleocapsid protein induces actin reorganization and apoptosis in COS-1 cells in the absence of growth factors, Biochem. J. 383 (2004) 13–18.

Rapid Genome Sequencing of RNA Viruses

Tetsuya Mizutani,* Daiji Endoh,† Michiko Okamoto,‡ Kazuya Shirato,* Hiroyuki Shimizu,* Minetaro Arita,* Shuetsu Fukushi,* Masayuki Saijo,* Kouji, Sakai,* Chang Kweng Lim,* Mikako Ito,* Reiko Nerome,* Tomohiko Takasaki,* Koji Ishii,* Tetsuro Suzuki,* Ichiro Kurane,* Shigeru Morikawa,* and Hidekazu Nishimura‡

We developed a system for rapid determination of viral RNA sequences whereby genomic sequence is obtained from cultured virus isolates without subcloning into plasmid vectors. This method affords new opportunities to address the challenges of unknown or untypeable emerging viruses.

Over the past few years, global migration has led to emerging infectious diseases that pose substantial risks to public health. To prevent potential outbreaks, early detection of infectious pathogens is necessary. In particular, the recent outbreak of severe acute respiratory syndrome (SARS) provided important lessons on how unknown viruses should be detected rapidly. Thus, a standardized and qualified system is required for rapid nucleic acid sequence determination for newly emerging viruses.

Recently, we developed a new method for detecting RNA viruses. This method, based on cDNA representational difference analysis (cDNA RDA), uses 96 hexanucleotides that are not suitable for priming ribosomal RNAs but that normally prime most of the genome of an RNA virus as primers for reverse transcription in cDNA RDA (*1*). However, the RDA method with a cloning step requires at least 1 week for the determination of the nucleic acid sequence.

The Method

Our new system for rapid determination of viral RNA sequence (RDV) uses whole-genome amplification and direct sequencing techniques (Figure 1). The RDV method comprises 6 procedures: 1) effective destruction of cellular RNA and DNA for semipurification of viral particles, 2) effective elimination of DNA fragments by using a prefiltration column system and elution of small amounts of RNA, 3) effective synthesis of first- and second-strand cDNAs, 4) construction and amplification of a cDNA library, 5) construction of a second cDNA library, and 6) direct sequencing using optimized primers. The RDV method enables a broad range of partial nucleotide sequences within the entire viral RNA genome to be obtained within 2 days without cloning into plasmids.

To eliminate contaminating cellular RNA and DNA from the samples, 0.001 μg of RNase A (Qiagen, Hilden, Germany) and 1 μL (2 U) of Turbo DNA-free DNase I (Ambion, Austin, TX, USA) with 1× Turbo DNA-free buffer were incubated at 37°C for 30 min under conditions that prevented destruction of viral RNA in the viral particles. The RNA in the viral particles was then extracted within 30 min by using a total RNA isolation mini kit (Agilent Technologies Inc., Palo Alto, CA, USA). We confirmed that DNA was effectively eliminated by this RNA extraction kit.

In accordance with the Invitrogen manual, cDNA was synthesized, by using random hexamers (Takara Bio Inc., Kyoto, Japan) and Superscript III (Invitrogen, Carlsbad, CA, USA) lacking RNase H activity, at 50°C for 1 h. Then 60 U of RNase H (Takara Bio Inc.) added before synthesis of second-strand cDNA at 50°C for 1 h. In accordance with the manual, a whole genome amplification system (WGA; Sigma-Aldrich, Saint Louis, MO, USA), which was developed for amplification of genomic DNA, was used to amplify viral double-stranded cDNA. This process was

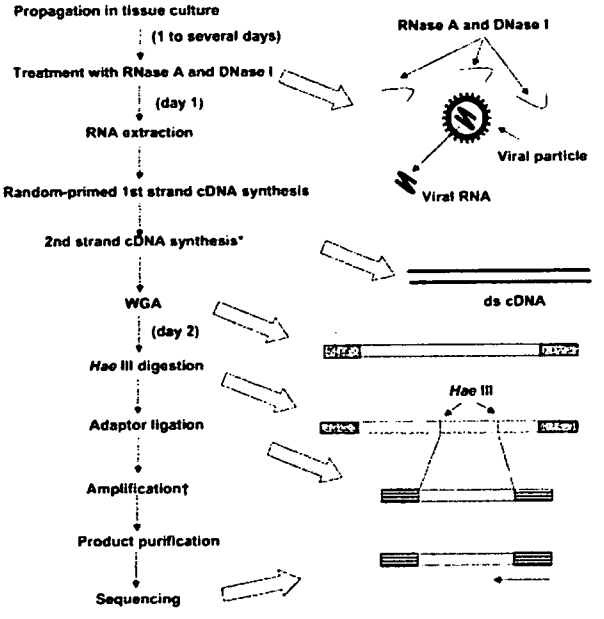

Figure 1. Overall scheme of the rapid determination of viral RNA sequence method. *By adding RNase H; WGA, whole genome amplification; †With specially designed primer sets as shown in Figure 2.

*National Institute of Infectious Diseases, Tokyo, Japan; †Rakuno Gakuen University, Ebetsu, Japan; and ‡Sendai Medical Center, Sendai, Japan

performed within 90 min. Instead of the Taq polymerase recommended in the kit, we used 1.25 U of AmpliTaq Gold LD (Applied Biosystems, Foster City, CA, USA) to obtain a high yield of the PCR products. Primers were provided in the WGA kit, but no information regarding their sequences was obtained. The reaction mixture was heated at 95°C for 9 min (for activation of AmpliTaq Gold), followed by 70 cycles of amplification using Mastercycler (Eppendorf AG, Hamburg, Germany). Each PCR cycle consisted of annealing at 68°C for 1 min, primer extension at 72°C for 5 min, and denaturation at 94°C for 1 min.

The 1st cDNA library was digested with 40 U of *Hae*III (Takara Bio Inc.) at 37°C for 30 min. DNA was purified by using the MonoFas DNA isolation system (GL Science, Tokyo, Japan), and a blunt *EcoR*I-*Not*I-*Bam*HI adaptor (10 pmol; Takara Bio Inc.) was ligated at 16°C for 30 min by using DNA Ligation Kit, Mighty Mix (Takara Bio Inc.). The second cDNA library was amplified by PCR with specially designed primer sets in which 6 nucleotides composed of CC (*Hae*III-digested sequence) and 4 variable nucleotides were added to the 3′ end of the adaptor sequence (Figure 2). For example, 1 primer set was as follows: forward primer, H1–1: 5′-AATTCGGCGGCCGCG GATCC*CC*GGGG-3′; reverse primer H9–3: 5′-AATT CGGCGGCCGCGGATCC*CC*AGGA-3′ (the adaptor sequence is underlined, and the *Hae*III-digested sequence is shown in italics) (Figure 2).

We always used >12 primer sets and 0.83 μmol of each primer per cDNA library. PCR was performed with AmpliTaq Gold Master Mix (Applied Biosystems). The reaction mixture was heated at 95°C for 12 min, followed by 70 cycles of amplification. Each PCR cycle consisted of annealing and primer extension at 72°C for 30 s and denaturation at 94°C for 30 s. A single band was consistently obtained in ≈50% of the reactions. DNA was purified from the PCR by using MonoFas. Occasionally, we purified DNA fragments from the gels when >2 bands were detected. Direct sequencing was performed with the forward primer, reverse primer, or both.

When the number of viral particles in the sample was high, we omitted the RNase A and DNase I treatments and used the RNeasy Mini Kit (Qiagen) for RNA extraction. We occasionally used a whole transcriptome amplification kit (Rubicon Genomics Inc, Ann Arbor, MI, USA) instead of the WGA kit because both kits yielded similar amplification results.

In preliminary studies that used referential RNA viruses, we attempted to determine the nucleic acid sequences of SARS coronavirus, mouse hepatitis virus, West Nile virus, Japanese encephalitis virus, and dengue virus type 2 in culture supernatants (10–100 μL) by using the RDV method. The percentages of positive fragments (number of fragments containing viral nucleic acid/total number of

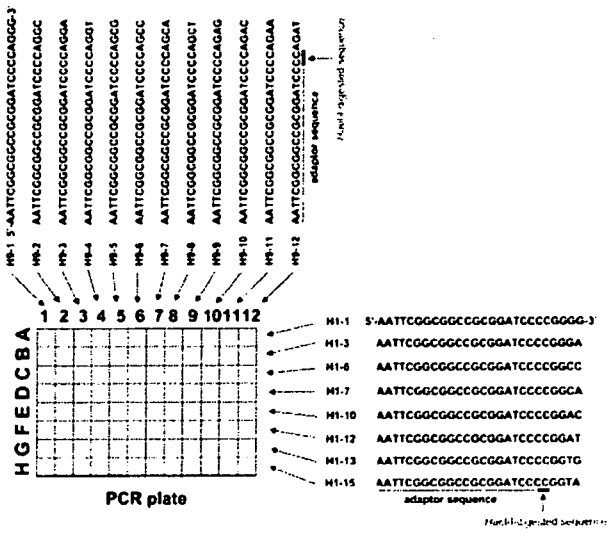

Figure 2. Primers used in rapid determination of viral RNA sequence method.

sequenced fragments) in the reactions for detection of these 5 viruses were 60% (3/5), 45% (5/11), 100% (12/12), 50% (5/10), and 40% (4/10), respectively. As a clinical application, a throat swab specimen from a patient with fever and upper respiratory infection was characterized. Although the specimen exhibited enterovirus-like cytopathic effect by inoculation into HEF and GMK cells when cell culture system for virus isolation was used (*2*), extracted RNA from the supernatant of the cells showed no amplification by reverse transcription–PCR (RT-PCR) when 1 of the conventional primer sets for human enteroviruses was used (*3*,*4*). In the cell culture supernatant analysis by the RDV method, the specimen exhibited amplification of the partial nucleotide sequences of coxsackie A14 virus (nucleotide sequence data are available in the DDBJ/EMBL/GenBank databases under accession nos. AB275848–AB275853). Thus, the RDV method could detect unidentified cytopathic-effect agents such as enterovirus that could not be detected by RT-PCR when the conventional primer set for enteroviruses was used.

Conclusions

The RDV method is a rapid method for the direct determination of viral RNA sequences without using the cDNA cloning procedure. The limitations of the RDV method are the requirement for cell culture isolate and the large number of steps. However, RDV would be useful for species-independent detection of RNA viruses including unknown or untypeable emerging RNA viruses. Furthermore, with minor modifications, this method would also be applicable to the detection of DNA viruses and bacteria.

Acknowledgments

We thank F. Taguchi and R. Watanabe for helpful discussions and M. Ogata for assistance.

This work was supported in part by the Japan Society for Promotion of Science, Tokyo, Japan.

Dr Mizutani is a senior researcher at the National Institute of Infectious Diseases, Tokyo, Japan. His current research focus is infectious disease surveillance by using new technologies.

References

1. Endoh D, Mizutani T, Kirisawa R, Maki Y, Saito H, Kon Y, et al. Species-independent detection of RNA virus by representational difference analysis using non-ribosomal hexanucleotides for reverse transcription. Nucleic Acids Res. 2005;33:e65.
2. Numazaki Y, Oahima T, Ohmi A, Tanaka A, Oizumi Y, Komatsu S, et al. A microplate method for isolation of viruses from infants and children with acute respiratory infections. Microbiol Immunol. 1987;31:1085–95.
3. Olive DM, Al-Mufti S, Al-Mulla W, Khan MA, Pasca A, Stanway G, et al. Detection and differentiation of picornaviruses in clinical samples following genomic amplification. J Gen Virol. 1990;71:2141–7.
4. Ishiko H, Shimada Y, Yonaha M, Hashimoto O, Hayashi A, Sakae K, et al. Molecular diagnosis of human enteroviruses by phylogeny-based classification by use of the VP4 sequence. J Infect Dis. 2002;185:744–54.

Address for correspondence: Tetsuya Mizutani, Department of Virology 1, National Institute of Infectious Diseases, Gakuen 4-7-1, Musashimurayama City, Tokyo 208-0011, Japan; email: tmizutan@nih.go.jp

JOURNAL OF VIROLOGY, Nov. 2006, p. 11265–11273 Vol. 80, No. 22
0022-538X/06/$08.00+0 doi:10.1128/JVI.01203-06

Oligomerization of Hepatitis C Virus Core Protein Is Crucial for Interaction with the Cytoplasmic Domain of E1 Envelope Protein▽

Kousuke Nakai,[1] Toru Okamoto,[1] Tomomi Kimura-Someya,[2] Koji Ishii,[2] Chang Kweng Lim,[1] Hideki Tani,[1] Eiko Matsuo,[1] Takayuki Abe,[1] Yoshio Mori,[1] Tetsuro Suzuki,[2] Tatsuo Miyamura,[2] Jack H. Nunberg,[3] Kohji Moriishi,[1] and Yoshiharu Matsuura[1]*

Department of Molecular Virology, Research Institute for Microbial Diseases, Osaka University, Osaka,[1] Department of Virology II, National Institute of Infectious Diseases, Tokyo,[2] Japan, and Montana Biotechnology Center, The University of Montana, Missoula, Montana 59812[3]

Received 9 June 2006/Accepted 28 August 2006

Hepatitis C virus (HCV) contains two membrane-associated envelope glycoproteins, E1 and E2, which assemble as a heterodimer in the endoplasmic reticulum (ER). In this study, predictive algorithms and genetic analyses of deletion mutants and glycosylation site variants of the E1 glycoprotein were used to suggest that the glycoprotein can adopt two topologies in the ER membrane: the conventional type I membrane topology and a polytopic topology in which the protein spans the ER membrane twice with an intervening cytoplasmic loop (amino acid residues 288 to 360). We also demonstrate that the E1 glycoprotein is able to associate with the HCV core protein, but only upon oligomerization of the core protein in the presence of tRNA to form capsid-like structures. Yeast two-hybrid and immunoprecipitation analyses reveal that oligomerization of the core protein is promoted by amino acid residues 72 to 91 in the core. Furthermore, the association between the E1 glycoprotein and the assembled core can be recapitulated using a fusion protein containing the putative cytoplasmic loop of the E1 glycoprotein. This fusion protein is also able to compete with the intact E1 glycoprotein for binding to the core. Mutagenesis of the cytoplasmic loop of E1 was used to define a region of four amino acids (residues 312 to 315) that is important for interaction with the assembled HCV core. Taken together, our studies suggest that interaction between the self-oligomerized HCV core and the E1 glycoprotein is mediated through the cytoplasmic loop present in a polytopic form of the E1 glycoprotein.

Hepatitis C virus (HCV) is the causative agent of chronic hepatitis C, leading to steatosis, cirrhosis, and hepatocellular carcinoma. It is estimated that over 170 million people are infected with HCV worldwide (5, 18, 37). HCV is an enveloped single-stranded plus-sense RNA virus in the *Hepacivirus* genus of the family *Flaviviridae*, which also includes the flaviviruses and pestiviruses (36). The genome of HCV encodes a polyprotein of approximately 3,000 amino acids which is cotranslationally and posttranslationally processed to generate at least 10 viral proteins (12). The structural proteins, the core and E1 and E2 envelope glycoproteins, are encoded in the N-terminal portion of the polyprotein, and the nonstructural proteins, thought to be required for replication of the viral genome, are encoded in the C-terminal region (11). The core protein, which interacts with viral RNA (47) to form the nucleocapsid, is liberated from the N terminus of the polyprotein by signal peptidase cleavage in the downstream E1 protein (at position 191), and the C-terminal transmembrane region of the core protein (residue 164 to 191) is further cleaved at residues 177 or 179 by the signal peptide peptidase (16, 43). The remaining hydrophobic region of the core protein (domain II; residues 119 to 174) has been shown to affect the efficiency of signal peptide peptidase cleavage and the intracellular localization of core protein (14, 44). Although the C-terminal transmembrane region of core protein and E1 were reported to interact with each other within the intramembrane space (25), the central hydrophobic region from residues 119 to 152 within domain II was also suggested to be responsible for the interaction between core and E1 (27).

Recently, in vitro replication of a JFH1 clone of HCV genotype 2a derived from a patient with fulminant hepatitis C was reported in a cell line that had been cured of its HCV replicon by treatment with interferon (23, 50, 51). However, this reverse genetics system is limited to the JFH-1 clone of genotype 2a and specific cell lines. Robust and reliable in vitro replication of other major genotypes of HCV such as genotypes 1a and 1b has yet to be developed. So far, biological functions of HCV envelope proteins have been characterized by using recombinant envelope proteins expressed in vitro, HCV-like particles produced in insect cells, and the pseudotyped virions based on vesicular stomatitis virus and retroviruses (8). The HCV polyprotein precursor must be specifically threaded through the membrane of the endoplasmic reticulum (ER) to undergo maturation to form the mature envelope glycoproteins (7). In the polyprotein, the C-terminal regions of E1 and E2 each contain a membrane-spanning domain as well as the hydrophobic signal peptide of the downstream viral protein (E2 and p7, respectively). These domains form hairpin structures that pass through the membrane twice, to allow processing by signal peptidase in the ER lumen. Upon signal peptidase cleavage, the C termini are thought to translocate into the cytoplasm to generate the type I membrane topology of the mature glycoproteins. The mature E1 and E2 glycoproteins

* Corresponding author. Mailing address: Department of Molecular Virology, Research Institute for Microbial Diseases, Osaka University, 3-1, Yamadaoka, Suita, Osaka 565-0871, Japan. Phone: 81-6-6879-8340. Fax: 81-6-6879-8269. E-mail: matsuura@biken.osaka-u.ac.jp.

▽ Published ahead of print on 13 September 2006.

remain noncovalently associated, interacting in part through their C-terminal transmembrane domains, which also mediate retention of the E1-E2 complex in the ER. Based on this model of membrane topology, the HCV envelope glycoproteins possess little or no cytoplasmic region. However, a physical association between E1 and the cytosolic core protein has been reported (25, 27), suggesting that the E1 glycoprotein is able to expose a cytoplasmic domain of sufficient length to interact with the core. In addition, the presence of the core protein has been shown to affect the folding of E1 (32).

We have previously suggested that the E1 glycoprotein may adopt a polytopic (double membrane-spanning) topology that coexists with the dominant type I form (35). In this study, we provide genetic evidence for a polytopic form of the E1 glycoprotein and for exposure of a centrally located cytoplasmic domain. Furthermore, we show that the cytoplasmic region of the polytopic form of E1 is required for interaction with amino acid residues 72 to 91 of the core protein.

MATERIALS AND METHODS

Cell culture. 293T cells were maintained in Dulbecco's modified Eagle's medium (Sigma, St. Louis, MO) containing 2 mM L-glutamine, penicillin, and streptomycin and supplemented with 10% fetal bovine serum.

Plasmids. A cDNA of E1 glycoprotein was amplified from HCV type 1b strain J1 (1) by PCR using *Pfu* Turbo DNA polymerase (Stratagene, La Jolla, CA) and inserted between NheI and BamHI sites of pJW4303, which contains the signal sequence of tissue plasminogen activator and the bovine growth hormone polyadenylation signal (a kind gift from J. M. Mullins), to generate pJW383. For the deletion analysis, the plasmids pJW360 and pJW288 encoding residues 192 to 360 and 192 to 288, respectively, were amplified by PCR and cloned into pJW4303. The plasmids pJW383d1 and pJW383d2, containing deletions in residues 261 to 286 and 289 to 340, respectively, were generated from pJW383 by splicing of overlapping extensions (13, 15) as described previously (44). A cDNA fragment encoding core to E2 proteins of HCV strain J1 was amplified by PCR and cloned into pCAGGs-PUR (28), and glycosylation site mutations in the E1 protein were generated by the method of splicing by overlapping extension. For the yeast two-hybrid assay, pGBKT7HCVCore173 was used as bait, as described previously (38). The gene encoding amino acids 288 to 346 of HCV E1 protein was amplified from cDNA of strain J1 and introduced into NdeI and EcoRI sites of a pGADT7 vector (Clontech, Palo Alto, CA). In the same way, deletion mutants of core protein encoding residues 1 to 151, 1 to 25, 24 to 173, 38 to 173, 58 to 173, 72 to 173, and 92 to 173 were amplified by PCR and cloned into a pGBKT7 vector. The FLAG sequence was introduced between amino acids 195 and 196 of the cDNA encoding residues 1 to 383 of the HCV polyprotein and replaced Ala^{383} with Arg to avoid processing by signal peptidase and spacer amino acids (Gly-Gly-Gly-Ser), and influenza virus hemagglutinin (HA) sequence was added at the C terminus. The resulting cDNA fragment encoding core protein, FLAG tag, E1, and HA tag was cloned into a pcDNA3.1(+) vector and designated Flag-core-E1-HA (see Fig. 2D, below) and used for in vitro transcription and translation. Similarly, the FLAG sequence was introduced into the cDNA encoding residues 151 to 383 of the HCV polyprotein, and the HA sequence was added at the C terminus. The resulting cDNA fragment encoding the C-terminal hydrophobic/transmembrane region of the core protein, FLAG tag, E1, and HA tag was designated Flag-E1-HA (see Fig. 3A, below). The DNA fragments encoding residues 1 to 191 with amino acids 72 to 91 deleted were generated by splicing via overlapping extension and cloned into pCAGGS (CoreΔ72-91) (see Fig. 4A, below) (42). The DNA fragment encoding the cytoplasmic domain of the E1 protein with a C-terminal HA tag was amplified by PCR and introduced at HindIII and SacII sites of pEGFP-C3. pCAGGS plasmids encoding core to p7 replacing residues 304 to 307, 308 to 311, 312 to 315, 316 to 319, 320 to 323, 324 to 327, or 328 to 331 with Ala were generated by using splicing with overlapping extension (see Fig. 6A, below).

Antibodies. Mouse monoclonal antibody to HA tag (HA11) and anti-FLAG antibody (M2) were purchased from Covance (Richmond, CA) and Sigma, respectively. Mouse monoclonal antibodies to core protein (clones 11-7, 11-10, and 11-14) were gifts from S. Yagi (2). Anti-E1 mouse monoclonal antibody (clone 0726) was prepared by immunization using the membrane fraction of the CHO L10 cell line, which constitutively expresses HCV envelope proteins (30). Anti-E2 monoclonal antibody (clone 187) was a generous gift from M. Kohara.

Yeast two-hybrid assay. A yeast two-hybrid assay was carried out by using Matchmaker system 3 (Clontech) according to the manufacturer's protocol. The bait vector pGBKT7HCVcore 173 (38) or empty plasmid was transfected into *Saccharomyces cerevisiae* strain AH109 together with the prey vectors, pGADT7-based constructs (see Table 1, below). The yeast cells possessing pGBKT7/p-53 and pGADT7/large T antigen were used as positive controls, while yeast cells possessing pGBKT7 and pGADT7 were the negative controls. These transfected yeast colonies were cultivated on dropout plates lacking Trp, Leu, His, and Ade (test plates) or plates lacking Trp and Leu (control plates) and then incubated at 30°C for 1 week.

Transfection, immunoblotting, and immunoprecipitation. Liposome-mediated DNA transfection using Lipofectamine 2000 (Invitrogen, Carlsbad, CA) was described previously (38). Transfected cells were cultured at 2×10^5 cells/well in a six-well plate, harvested 30 to 48 h posttransfection, washed twice with phosphate-buffered saline (PBS), and incubated at 4°C for 30 min in 0.25 ml of lysis buffer (20 mM Tris-HCl [pH 7.4], 135 mM NaCl, 1% Triton X-100, and 10% glycerol supplemented with 1 mM phenylmethylsulfonyl fluoride, 50 mM NaF, and 5 mM Na_3VO_4). After freezing and thawing, lysed cells were centrifuged at $20,000 \times g$ for 5 min. The resulting cleared lysate was stored at −80°C prior to use for immunoprecipitation and blotting. Immunoprecipitation was carried out according to the method described previously (44). Briefly, lysates were preincubated at 4°C for 5 h in the lysis buffer with or without 1 mM $MgCl_2$ and 0.1 mg/ml of yeast tRNA (Sigma) prior to immunoprecipitation. The resulting lysates (0.2 ml) were gently rotated with 1.0 μg of anti-FLAG, anti-HA, or mixed mouse monoclonal anti-HCV core antibodies or mouse monoclonal antibody to the E1 protein at 4°C for 3 h with or without 1 mM $MgCl_2$ and 0.1 mg/ml of yeast tRNA. The immunocomplex was gently rotated at 4°C for 3 h with 10 μl of 50% (vol/vol) protein G-Sepharose 4 Fast Flow beads (Amersham Pharmacia Biotech, Franklin Lakes, NJ) with or without 1 mM $MgCl_2$ and 0.1 mg/ml of yeast tRNA and then centrifuged at $20,000 \times g$ for 30 s. The precipitated beads were washed five times with 0.5 ml of lysis buffer containing or lacking 1 mM $MgCl_2$ and 0.1 mg/ml of yeast tRNA and then boiled in 50 μl of the loading buffer. The boiled samples were subjected to sodium dodecyl sulfate-polyacrylamide gel electrophoresis. The proteins in gels were transferred to Immobilon-P polyvinylidene difluoride membranes (Millipore, Bedford, MA) and then blotted with primary antibody and secondary horseradish peroxidase-conjugated antibody. The immunocomplexes on membranes were visualized with Super Signal West Femto substrate (Pierce, Rockford, IL) and detected by using an image analyzer LAS-3000 (Fujifilm, Tokyo, Japan).

Protease protection assay of HCV proteins synthesized by in vitro transcription/translation. A plasmid encoding a FLAG-core-E1-HA protein was transcribed under the control of a T7 promoter by using the RiboMax large-scale RNA production system with Ribo m^7G cap analog (Promega, Madison, WI). In vitro translation was carried out in the presence of [^{35}S]methionine-cysteine (Amersham, Piscataway, NJ) by using rabbit reticulocyte lysate and canine pancreatic microsomal membrane (Promega). Translated sample was diluted sevenfold with PBS and then mixed with tosylsulfonyl phenylalanyl chloromethyl ketone-treated trypsin (Sigma) at a final concentration of 2 μg/ml. The mixture was incubated at 30°C for 60 min with or without 0.5% Nonidet P-40, and then soybean trypsin inhibitor (Sigma) was added at a final concentration of 20 μg/ml. Digestion products were immunoprecipitated with anti-FLAG antibody.

Indirect immunofluorescence analysis. 293T cells were washed with PBS at 40 h after transfection and fixed with 3% paraformaldehyde in PBS for 20 min at room temperature. The fixed cells were permeabilized with 0.2% Triton X-100 for 3 min at room temperature and blocked with nonfat milk solution. Cells were incubated with the anti-E1 antibody for 60 min at 37°C and then with fluorescein isothiocyanate-conjugated goat anti-mouse immunoglobulin G (IgG; TAGO, Burlingame, CA). HCV E1 protein was visualized by fluorescence microscopy (TE300; Nikon, Tokyo, Japan).

Velocity sedimentation with sucrose gradients. Transfected 293T cell were suspended in MNT buffer (20 mM 2-morpholinoethanesulfonic acid, 100 mM NaCl, 30 mM Tris-HCl [pH 8.6], and 0.1% Triton X-100) and then incubated at 4°C for 5 h with or without 0.1 mg/ml of yeast tRNA and 1 mM $MgCl_2$. Each sample was layered on top of 12 ml of sucrose with a 20 to 60% gradient and then centrifuged in a Beckman SW 41Ti rotor (Beckman Coulter, Tokyo, Japan) at 30,000 rpm for 3 h at 4°C. Centrifuged lysates were collected from the bottoms of the tubes and then concentrated with trichloroacetic acid. After washing with ethanol, concentrated proteins were subjected to SDS-PAGE and immunoblotting.

RESULTS

Prediction of the topology of the E1 protein in the membrane. Although a small fraction of the HCV envelope glycoproteins expressed in 293T cells is translocated onto the plasma membrane (3), the vast majority of E1 is retained in the ER membrane (6). Previously, we showed that both a central hydrophobic region of E1 (residues 260 to 288) and the C-terminal transmembrane domain (residues 360 to 383) are important for ER retention (29). As in the C-terminal hydrophobic region, the amino acid sequence of the central hydrophobic region is highly conserved among HCV isolates (4). To investigate the role of these two hydrophobic regions in the biogenesis of the E1 glycoprotein, we utilized the TMHMM algorithm (19), a computer program trained to identify potential transmembrane helical regions. The algorithm identified both hydrophobic regions as having a high probability of transmembrane helix (Fig. 1A). To examine the function of the hydrophobic regions as transmembrane domains, we constructed a series of deletion mutants in the E1 protein in which one or the other of the hydrophobic segments was absent (Fig. 1B). Mutant E1 glycoproteins were expressed in 293T cells, and the cellular localization of E1 proteins was determined by indirect immunofluorescence analysis (Fig. 1B). The full-length E1 (383) was detected only in permeabilized cells, consistent with its retention in the ER. The 383d2 mutant, which contains both hydrophobic regions but lacks the intervening hydrophilic region (residues 289 to 340), was also detected in the cytoplasm but not on the cell surface as the full-length E1. By contrast, deletion mutants lacking the central (383d1) or C-terminal (288 and 360) hydrophobic domains were detected on the cell surface in nonpermeabilized cells, suggesting that both the central and the C-terminal hydrophobic domains are required for retention of the E1 protein on the ER membrane. If the central hydrophobic domain traverses the ER membrane as predicted by the TMHMM program, the region between positions 288 and 360 would be expected to lie in the cytoplasmic space. Based on this model and on the results with E1 deletion mutants, we suggest that the E1 protein might be able to retain two membrane topologies: the conventional type I topology and a polytopic topology that spans the membrane twice with N and C termini in the ER lumen and an intervening cytoplasmic loop, as reported previously (35) (Fig. 1C). Recently, a similar polytopic form of the fusion glycoprotein of Newcastle disease virus was identified (31).

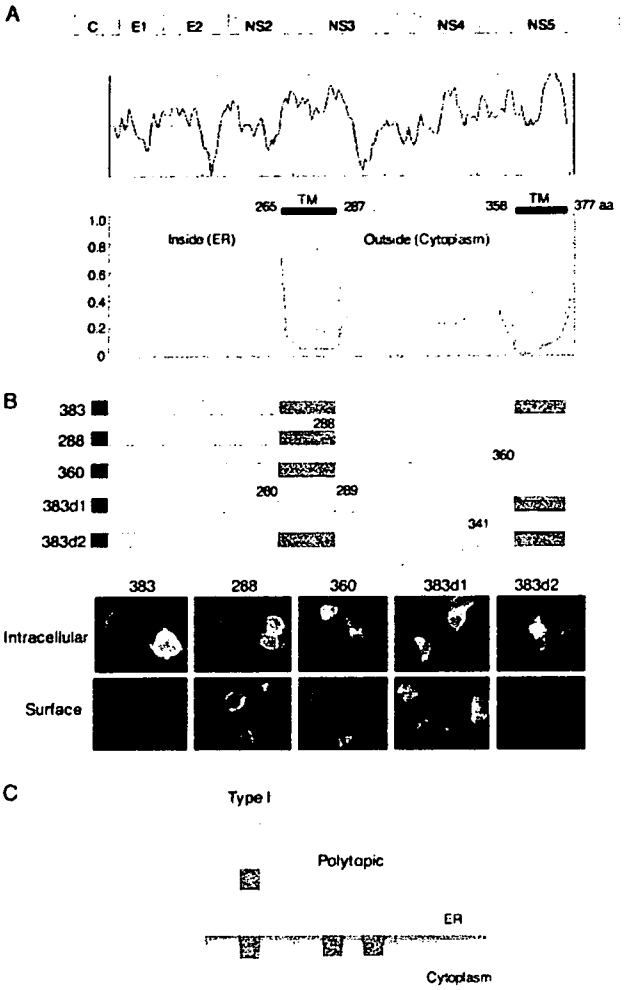

FIG. 1. Prediction of the membrane topology of the E1 protein. (A) Genome structure of HCV and a hydrophobic profile of the amino acid sequence of the E1 protein are shown at the top. The transmembrane helices in the E1 protein were predicted by the TMHMM program (19), and regions of high probability (amino acid residues 265 to 287 and 358 to 377) are indicated. (B) 293T cells transfected with the wild type (383) and deletion constructs were fixed with paraformaldehyde and permeabilized with Triton X-100 (intracellular) or not permeabilized (surface). E1 proteins were visualized with an anti-E1 monoclonal antibody and fluorescein isothiocyanate-conjugated anti-mouse IgG. (C) Possible topologies of the E1 protein on the ER. (Left) Type I topology model possessing a C-terminal transmembrane region; (right) a polytopic topology that spans the membrane twice, with both N and C termini in the ER lumen and with an intervening cytoplasmic loop.

Mutational analysis of putative N-glycosylation sites of the E1 glycoprotein. To explore the membrane topologies of E1, we examined the utilization of potential glycosylation sites. The E1 protein of HCV strain J1 (1) contains seven N-glycosylation sequence motifs (Asn-X-Ser/Thr) at amino acid positions 196, 209, 233, 234, 250, 305, and 325 (Fig. 2A). The Asn residues at these possible N-glycosylation sites were individually replaced with Gln, and the mutant E1 glycoproteins were expressed as a core-, E1-, or E2-containing polyprotein in 293T cells. In all cases, the mutant polyproteins were expressed and properly processed by signal peptidase and signal peptide peptidase to generate the core, E1, and E2 proteins (Fig. 2B). The mutant E1 proteins displayed distinct glycoforms consistent with changes in glycosylation. The wild-type E1 glycoprotein exhibited a major band of 34 kDa and a minor band of 32 kDa. The 325 mutant was unchanged from the wild-type E1, suggesting that the 325 position is not utilized, presumably due to an unfavorable NWSP motif in the genotype 1a protein (33). The 209, 233/234, and 250 mutants migrated faster than the authentic E1 protein and exhibited two bands of 32 and 30 kDa. The E1 of the 196 mutant was apparently not recognized by the monoclonal antibody directed to the N-terminal region of E1. In the 233 and 234 mutants, glycosylation occurred at the remaining Asn (234 or 233, respectively). These mutants comigrated with the wild-type E1 glycoforms, suggesting that

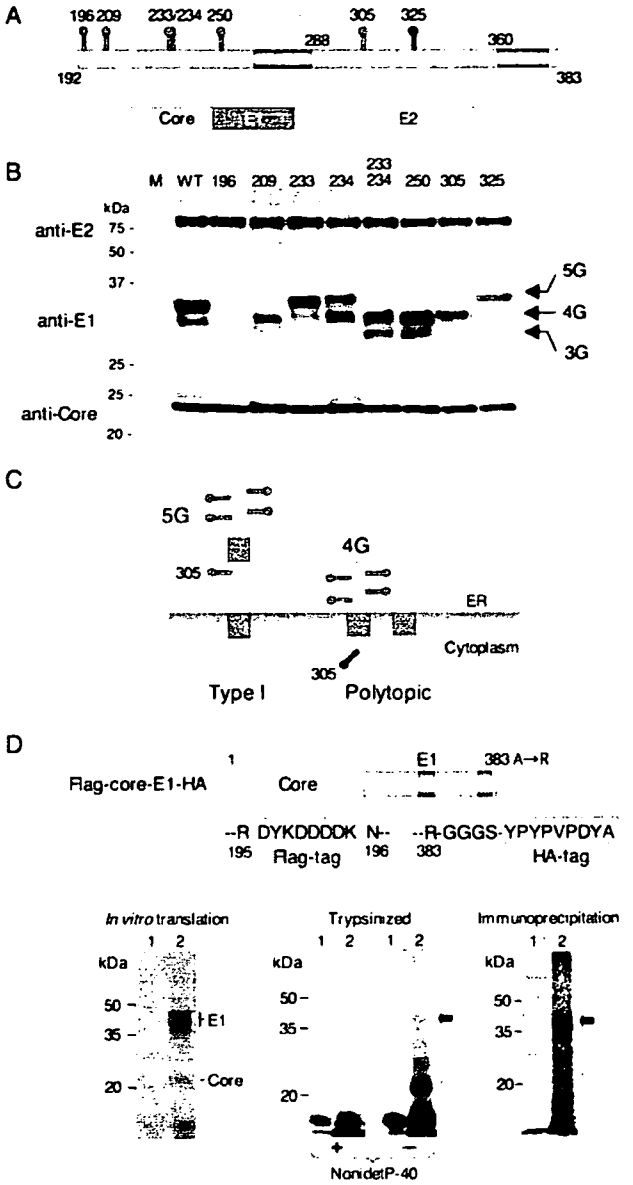

FIG. 2. Mutational analysis of N-glycosylation sites and protease protection assay of the E1 protein. (A) Positions of potential N-glycosylation sites (gray and black spikes) in the E1 protein are shown. (B) Asn residues in the possible N-glycosylation sites in the E1 protein were individually replaced with Gln. Mutant plasmids encoding the core, E1, and E2 polyproteins (A) were expressed in 293T cells, and processed core, E1, and E2 proteins were detected by immunoblotting. (C) Type I and polytopic topology models of E1 proteins bearing carbohydrates at positions of 196, 209, 234, 250, and 305 (5G) and 196, 209, 234, and 250 (4G), respectively. The 305 mutant would exhibit a single band of 4G irrespective of the topologic models. (D) Structure of the FLAG-core-E1-HA construct encoding the HCV core and E1 polyprotein carrying FLAG and HA tags in the N- and C-terminal regions of the E1 protein (top). (Bottom, left) In vitro translation of capped RNA transcribed from the FLAG-core-E1-HA (lane 2) and without RNA (lane 1) in the presence of [^{35}S]methionine-cysteine using rabbit reticulocyte lysate and canine pancreatic microsomal membrane. (Bottom, middle) Translated products of FLAG-core-E1-HA (lane 2) and without RNA (lane 1) were digested with trypsin in the presence (+) or absence (−) of 0.5% Nonidet P-40. (Bottom, right) Digestion products were immunoprecipitated with control (lane 1) and anti-FLAG (lane 2) antibody. Black and white arrows indicate protected and digested E1 protein, respectively.

only one or the other of the overlapping motifs can be utilized in the wild-type molecule. Glycosylation in this region was absent in the double mutant (233/234). The existence of two glycoforms of E1 may reflect incomplete and stochastic use of the available glycosylation sites or, alternatively, the presence of two discrete topological forms of E1 protein. For instance, the major band of 34 kDa in the wild-type glycoprotein might correspond to the type I topology form, with glycosylation at 196, 209, 234, 250, and 305 (5G), whereas the minor band of 32 kDa might correspond to the polytopic form of E1, bearing glycans at positions 196, 209, 234, and 250 (4G). In this regard, it is noteworthy that the 305 mutant of E1 exhibited only a single band of 32 kDa. The absence of a second glycoform is consistent with the putative cytoplasmic localization of Asn305 in a polytopic form of E1 (Fig. 2C). Taken together, this mutational analysis provides support to the model in which the HCV E1 glycoprotein is able to exist in either the type I or polytopic form. In the latter form, an extended cytoplasmic domain in E1 would be available to interact with the core protein in the virion.

Protease protection assay of the E1 protein. To confirm the presence of the cytoplasmic domain in the E1 protein, in vitro translation products of the HCV core and E1 polyprotein carrying FLAG and HA tags in the N- and C-terminal regions of the E1 protein, respectively, were digested with trypsin, and the protected portion of the E1 glycoprotein was immunoprecipitated by anti-FLAG antibody. As shown below in Fig. 4D, treatment of the translation products with trypsin in the presence of Nonidet P-40 resulted in complete digestion, and a 22-kDa band (major) and several <35-kDa faint bands were detected in the absence of the detergent. When in vitro-translated HCV core protein was treated similarly, no band was detected, irrespective of the presence of detergent (data not shown); therefore, the protected bands from trypsin digestion were derived from the E1 protein. Although the 22- to 35-kDa bands were specifically immunoprecipitated with anti-FLAG antibody but not with control antibody, the 35-kDa protein corresponding to the type I topology of the E1 protein resistant to trypsin digestion was dominant. This might be due to the difference in the reactivity of the anti-FLAG antibody, which recognizes the intact E1 protein more efficiently than digested ones. These results further support the presence of the polytopic form of HCV E1 glycoprotein, which has a cytoplasmic region together with a type I topology in the ER.

HCV core protein binds to the E1 protein in the presence of tRNA. The HCV core protein undergoes extensive conformational changes upon binding to nucleic acid and self-assembling into nucleocapsid-like particles (20). To investigate the effects of nucleic acid on oligomerization of the core protein, lysates of 293T cells expressing HCV core protein were incubated in the presence or absence of yeast tRNA (20) and subjected to velocity sedimentation in a sucrose gradient. Oligomerized core protein was detected in fractions 1 to 4 in the presence of tRNA but not in those in the absence of tRNA (Fig. 3A). To specifically examine the interaction between HCV core and E1 proteins in the assembly of the nucleocapsid-like particles, we coexpressed the core protein with an E1 protein possessing a FLAG tag near its N terminus and an HA tag at the C terminus (Flag-E1-HA) (Fig. 3B, left). The transfected cells were lysed with Triton X-100, and the E1 protein

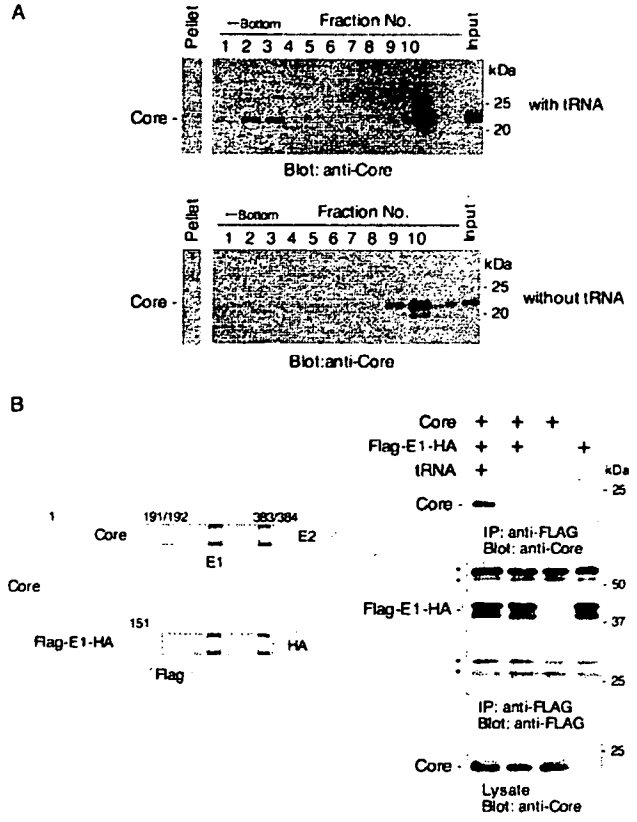

FIG. 3. HCV core protein binds to E1 protein in the presence of tRNA. (A) Cell lysates of 293T cells expressing HCV core protein were subjected to velocity sedimentation with a sucrose gradient in the presence or absence of tRNA. Oligomerized core protein was detected in fractions 1 to 4 in the presence of tRNA but not in those in the absence of tRNA. (B, left) cDNAs used for expression. FLAG-E1-HA encodes FLAG tag after the signal peptide and HA tag after the transmembrane region. (Right) Immunoprecipitation analyses. Cell lysates of 293T cells expressing core and FLAG-E1-HA proteins were immunoprecipitated by anti-FLAG antibody in the presence or absence of tRNA. The asterisks indicate nonspecific bands.

was immunoprecipitated by using an anti-FLAG antibody. Coprecipitation of core protein with E1 was assessed by Western blot analysis using a core-specific monoclonal antibody. Although HCV core protein was clearly coprecipitated with FLAG-E1-HA in the presence of tRNA, little association was seen in the absence of tRNA (Fig. 3B, right). Nonspecific precipitation of the core protein with tRNA was not observed (data not shown). Although a small amount of the intracellular core protein may already associate with viral RNA under the intracellular conditions, a large amount of RNA may be required for oligomerization that is detectable by the sedimentation assay. Together, our results suggest that tRNA facilitates oligomerization of the HCV core protein and potentiates the interaction between the core protein and E1.

The region spanning amino acid residues 72 to 91 in the HCV core protein is crucial for binding to the E1 protein in yeast. The interaction between the HCV core and E1 proteins likely occurs on the cytosolic side of the cell membrane and, thus, presumably involves the posited cytoplasmic loop region in the polytopic form of the E1 glycoprotein. To investigate the possibility for this specific interaction in cells, core protein lacking the transmembrane region (Core1-173) was examined for interaction with the putative E1 cytoplasmic loop region in a yeast two-hybrid system (Table 1). When Core1-173 was expressed with the E1 cytoplasmic region (residues 288 to 346), the yeast was able to grow on the dropout plate lacking Trp, Leu, His, and Ade, suggesting that the core protein associates with the cytoplasmic loop of the E1 protein in yeast. To determine the region of the HCV core protein responsible for the interaction with the cytoplasmic domain of E1, deletion mutants of the core were tested. Association in the yeast two-hybrid system was seen with Core24-173, Core38-173, Core58-173, Core72-173, and Core1-151 mutants, but not with Core92-173 and Core1-25. Nonspecific interaction of the GAL4 activation domain with these core mutants was not observed. These results suggest that the region spanning from amino acid residues 72 to 91 in the HCV core protein is important for interaction with the cytoplasmic domain of the E1 protein in yeast.

Amino acid residues 72 to 91 in the core protein are involved in oligomerization of the core protein and interaction with the E1 protein in mammalian cells. To examine the involvement of amino acid residues 72 to 91 of the HCV core protein in the interaction with the E1 protein in mammalian cells, FLAG-E1-HA was coexpressed with either a wild-type core or a deletion mutant lacking amino acid residues 72 to 91 (CoreΔ72-91) in 293T cells (Fig. 4A). Cell lysates were incubated with yeast tRNA, and FLAG-E1-HA was immunoprecipitated with anti-FLAG antibody. As shown in Fig. 4B (left), only the wild-type core protein, but not CoreΔ72-91, coprecipitated with E1. Self-oligomerization was also prevented by the deletion in CoreΔ72-91 (Fig. 4B, right). These results suggest that amino acid residues 72 to 91 in the HCV core protein play a crucial role in the interaction with the E1 protein and oligomerization of the core protein.

The E1 cytoplasmic domain interacts with the core protein in mammalian cells and inhibits the interaction with intact E1 protein in *trans*. To assess the involvement of the E1 cytoplasmic region in the interaction with core protein in mammalian

TABLE 1. Interaction between the core and the E1 cytoplasmic region in yeast

Bait	Growth with prey[a]			
	E1 cytoplasmic loop		No insert	
	Dropout	Control	Dropout	Control
Core1-173	+	+	−	+
Core24-173	+	+	−	+
Core38-173	+	+	−	+
Core58-173	+	+	−	+
Core72-173	+	+	−	+
Core92-173	−	+	−	+
Core1-151	+	+	−	+
Core1-25	−	+	−	+
No insert	−	+	−	+

[a] HCV core mutants were expressed as fusion proteins with the DNA binding region by using a bait plasmid. The HCV E1 cytoplasm region was expressed as a fusion protein with an activation domain by using a prey plasmid. Yeast growth was observed in dropout plates lacking Trp, Leu, Ade, and His (dropout) or plates lacking Trp and Leu (control). +, growth; −, no growth.

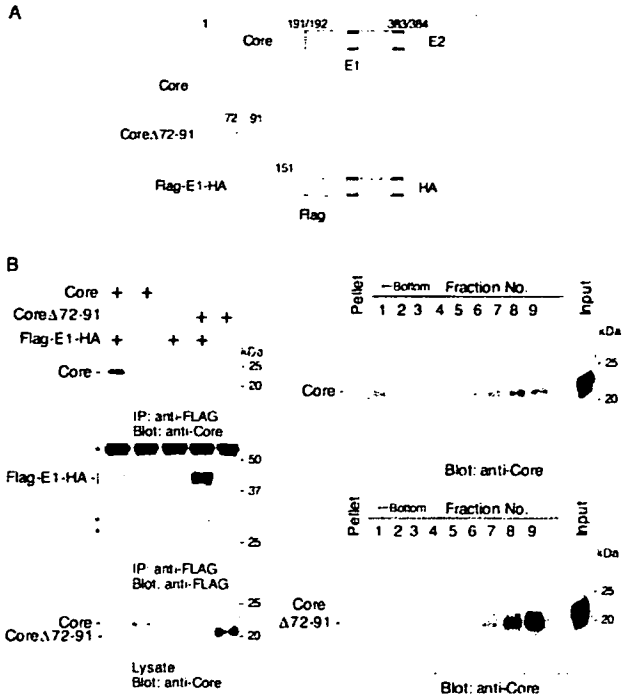

FIG. 4. Amino acid residues72 to 91 in the core protein are involved in oligomerization of the core protein and interaction with the E1 protein. (A) cDNAs used for expression. CoreΔ72-91 is an HCV core protein carrying a deletion of amino acid residues 72 to 91. (B, left) FLAG-E1-HA was coexpressed in 293T cells with either a wild-type core or CoreΔ72-91, and the interaction was analyzed by immunoprecipitation in the presence of tRNA. The asterisks indicate nonspecific bands. (Right) Oligomerization of a wild-type core or CoreΔ72-91 in the presence of tRNA. Wild-type core protein was self-oligomerized, but CoreΔ72-91 was not.

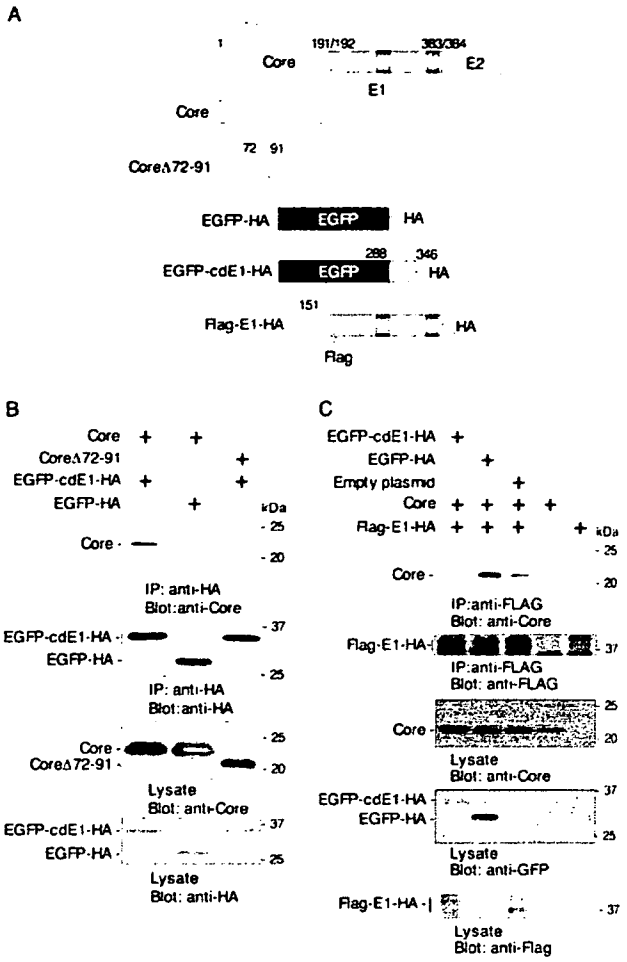

FIG. 5. Interaction of the E1 cytoplasmic loop with the core protein. (A) cDNAs used for expression. EGFP-cdE1-HA is an EGFP fusion protein carrying the E1 cytoplasmic region of amino acid residues 288 to 346 followed by an HA tag. (B) Wild-type core or CoreΔ72-91 was coexpressed with EGFP-cdE1-HA in 293T cells, and their interaction was analyzed by immunoprecipitation. EGFP-cdE1-HA coprecipitated with wild-type core protein, but not with CoreΔ72-91. (C) Inhibition of the interaction of the core protein with FLAG-E1-HA by expression of EGFP-cdE1-HA. Expression of EGFP-cdE1-HA but not of EGFP disrupted the interaction between core and E1 proteins.

cells, we constructed an enhanced green fluorescent protein (EGFP) fusion protein carrying the E1 cytoplasmic domain followed by an HA tag (EGFP-cdE1-HA) (Fig. 5A). Upon coexpression of EGFP-cdE1-HA with the wild-type core protein in 293T cells, the two proteins could be coprecipitated using anti-HA antibody (Fig. 5B). The mutant CoreΔ72-91 protein was unable to associate with EGFP-cdE1-HA (Fig. 5B). Together, these studies demonstrate that the cytoplasmic loop region of E1 is able to interact with the core protein and that core residues 72 to 91 are required for this association.

To further confirm the specificity of the interaction of the E1 cytoplasmic region with the core protein, we examined the ability of the EGFP-cdE1-HA protein to inhibit the association of the intact E1 protein (in Flag-E1-HA) with the wild-type core protein (Fig. 5C). Expression of EGFP-cdE1-HA but not EGFP-HA competed strongly with the interaction between core and the FLAG-tagged Flag-E1-HA protein. These results suggest that the cytoplasmic loop in the intact E1 glycoprotein can directly bind to HCV core protein. Interestingly, the EGFP-cdE1-HA protein was unable to inhibit this interaction in the context of the intact core and E1 and E2 polyproteins (data not shown), suggesting that expression of the core and E1 proteins in *cis* may prevent subsequent interaction with E1 expressed in *trans*.

Four amino acid residues, 312 to 315, in the cytoplasmic region of the E1 protein are important for interaction with the core protein. Alignment of the amino acid sequence of the E1 cytoplasmic region among different HCV genotypes revealed that the region from Gln^{302} to Pro^{328} is highly conserved (Fig. 6A). To determine residues in the E1 cytoplasmic region that are critical for interaction with the core protein, blocks of four residues each in the conserved region were replaced with Ala in the polyprotein (core, E1, E2, and p7) (Fig. 6A). These mutant polyproteins were expressed in 293T cells and immunoprecipitated with anti-core antibody; coprecipitated E1 protein was detected by immunoblotting using an anti-E1 monoclonal antibody (Fig. 6B). The replacement of four amino acid residues, 304 to 307, with Ala in the conserved region of the E1

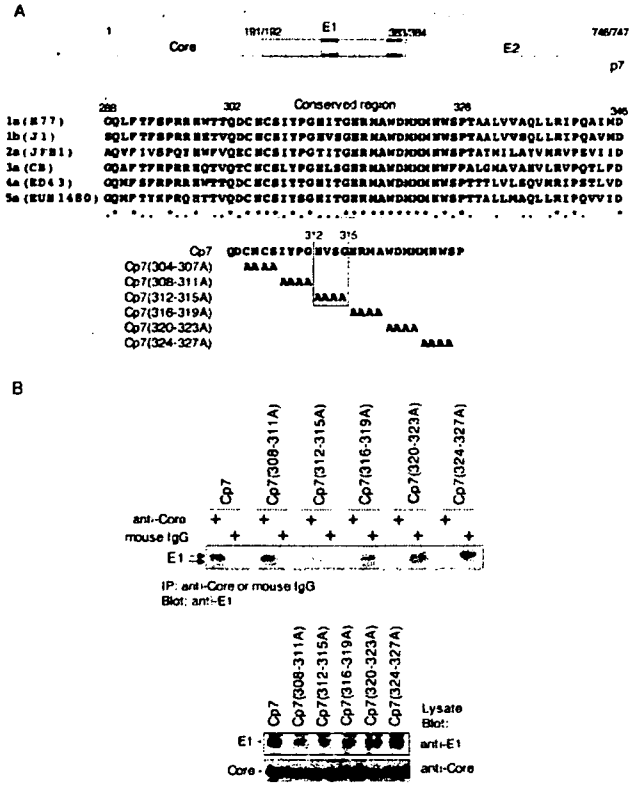

FIG. 6. Four amino acid residues, 312 to 315, in the cytoplasmic region of the E1 protein are important for interaction with the core protein. (A) Alignment of the amino acid sequence of the E1 cytoplasmic region among different HCV genotypes (1a, H77 [AF009606]; 1b, J1 [D89815]; 2a, JFH1 [AB047639]; 3a, CB [AF046866]; 4a, ED43 [Y11604]; 5a, EUH1480 [Y13184]). A conserved region from Gln^{302} to Pro^{328} is shown by gray shading. Mutant polyproteins consisting of the core, E1, E2, and p7 proteins with four residues each replaced by Ala in the conserved E1 region were constructed. Four amino acid residues, His^{312}, Val^{313}, Ser^{314}, and Gly^{315}, in the E1 cytoplasmic region of strain J1 and substitution of the amino acids with Ala in Cp7 (312-315A) are indicated by the box. (B) These mutant polyproteins were expressed in 293T cells and immunoprecipitated with anti-core antibody or nonspecific mouse IgG in the presence of $MgCl_2$ and tRNA. The E1 protein that coprecipitated with the core protein was detected by immunoblotting. The substitution of four amino acid residues, 304 to 307, with Ala in the conserved region of the E1 protein, Cp7 (304-307A), could not be examined due to the low level of expression.

protein could not be examined due to a low level of expression (data not shown). Among the mutant constructs examined, only the substitution at residues 312 to 315, Cp7 (312-315A), markedly diminished association with the core protein (Fig. 6B). These results suggest that this region in the E1 cytoplasmic domain of the J1 strain of HCV (His^{312}, Val^{313}, Ser^{314}, and Gly^{315}) is important for interaction with the core protein.

DISCUSSION

The biogenesis of the transmembrane glycoproteins involves a series of coordinated translation and membrane integration events that are directed by topogenic determinants within the nascent chains and that ultimately lead to the most favored topology for any given polypeptide (24). However, there is an increasing number of examples of glycoproteins that can assume multiple topological orientations. The large envelope protein of the hepatitis B virus, for instance, has been suggested to adopt distinct topologies that enable the protein to serve in virus assembly as a matrix-like protein and in virus entry as a receptor binding protein (22). An unglycosylated form of the HCV E2 protein has been identified and shown to interact with protein kinase R in the cytosol (45). In Newcastle disease virus, type I and polytopic forms of the fusion protein are present in the same cell, and the polytopic form is suggested to be involved in the membrane fusion event (31).

HCV glycoproteins E1 and E2 were shown to possess transmembrane domains and associate to form noncovalent heterodimers that are statically retained in the ER membrane upon recombinant expression (10, 29, 46). Previously, the E1 protein of genotype 1a was suggested to possess a single C-terminal transmembrane domain, based in part on its utilization of potential glycosylation sites (33) and on a model of the transmembrane domains of the E1 and E2 proteins, in which the C terminus reorients, upon signal peptidase cleavage, from the ER lumen to protrude slightly into the cytoplasm (7). In our study, we have suggested that the E1 protein can also adopt a polytopic topology in which the protein spans the ER membrane twice and includes an intervening cytoplasmic region. In this model, the membrane orientation of the C-terminal transmembrane region is inverted and translocation of the signal peptidase-cleaved C terminus is not required.

Our analysis revealed that the 305 mutant of the 1b genotype expressed by transfection exhibited a single band of 32 kDa, whereas that of genotype 1a expressed by recombinant vaccinia viruses has been reported to contain two bands (33). Although we do not know the reason for this discrepancy, it may relate to differences in the expression systems. HCV proteins expressed by vaccinia virus and Sindbis virus vectors formed disulfide-linked aggregates (9, 11, 34), and coexpression of a large amount of vaccinia viral proteins also may alter the proper processing of the expressed proteins, as suggested by Merola et al. (32). However, further work will be necessary to clarify the reasons for the differences in glycosylation patterns of E1 mutants obtained in the different expression systems.

Mottola et al. analyzed the determinants for ER localization of the E1 protein and showed that the juxtamembrane region of E1, between amino acid residues 290 and 333, was required for ER retention (41). This region lies within the ectodomain of the E1 protein in the type I topology and in the cytoplasmic region of the protein in the proposed polytopic form. ER localization determinants of transmembrane proteins have in general been located either in the cytosolic or in the transmembrane domain, not in the luminal ectodomain, except for the yeast Sec20 protein (41). Therefore, assignment of the ER localization signal to the cytoplasmic region of the E1 protein might further support the possibility of the polytopic topology model. Affinity purification and membrane reconstitution of the E1 protein carrying an affinity tag (S-peptide) in the putative cytoplasmic region are also consistent with this model (35). Together, these findings provide indirect support that the E1 glycoprotein can adopt a polytopic form.

As previously reported (20), oligomerization of the HCV core protein to form nucleocapsid-like particles requires the presence of stem-loop RNA structures, such as those in tRNA.

Here, we have demonstrated that self-assembly of the core protein occurs without envelope protein in the presence of tRNA and that tRNA is required for the association of E1 glycoprotein with the core protein, suggesting that oligomerization of the core protein may be a prerequisite for this interaction during virus assembly. Based on hydrophobicity and the clustering of basic amino acids, the HCV core protein is proposed to possess three domains: the N-terminal basic and hydrophilic region (domain 1; residues 1 to 118), a central basic and hydrophobic domain (domain 2; residues 119 to 174), and the hydrophobic signal sequence for E1 (domain 3; residues 175 to 191) (14). Biophysical characterization of the core protein indicated that the C-terminal residues 125 to 179 were critical for the folding and oligomerization of the core protein (21). Although our mutant HCV polyprotein containing Ala substitutions at residues 312 to 315 in the cytoplasmic region of the E1 protein exhibited a clear reduction in its interaction with the core protein, a substantial amount of residual binding was retained. These results suggest that regions other than the residues from 312 to 315 in the E1 protein are also involved in the interaction with the core protein.

In Semliki Forest virus, the cytoplasmic domain of the E2 glycoprotein, which corresponds to the E1 protein in HCV, has been shown to interact with the capsid protein (26, 49). Assembly of alphaviruses has also been found to require the specific interaction between the C-terminal cytoplasmic domain of the E2 protein and the capsid protein (17). Although the functional significance of the two forms of the HCV E1 protein is still unclear, the E1 cytoplasmic region among different HCV genotypes is well conserved and four amino acid residues, His^{312}, Val^{313}, Ser^{314}, and Gly^{315} of strain J1, were shown to be important for interaction with the core protein. Although the four amino acid sequences identified in strain J1 of genotype 1b are not strictly conserved among the different HCV genotypes (Fig. 6A), a pattern of polar-hydrophobic-polar-glycine residues can be discerned in all of them. The interaction of the cytoplasmic E1 protein with the core protein may indicate that the polytopic form is a mature E1 protein that is incorporated into virions.

In conclusion, the polytopic topology model of the HCV E1 protein and the interaction of oligomerized core protein with the cytoplasmic region of the E1 protein may provide clues to aid in understanding the biosynthesis and assembly of the HCV structural proteins. HCV core protein is also involved in the development of liver steatosis, type II diabetes mellitus, and hepatocellular carcinoma in transgenic mice (39, 40, 48). A detailed knowledge of the assembly of HCV particles will provide the basis for the development of effective therapeutics for chronic hepatitis C.

ACKNOWLEDGMENTS

We gratefully thank H. Murase for secretarial work.

This work was supported in part by grants-in-aid from the Ministry of Health, Labor, and Welfare, the Ministry of Education, Culture, Sports, Science, and Technology, the 21st Century Center of Excellence Program, and the Foundation for Biomedical Research and Innovation.

REFERENCES

1. **Aizaki, H., Y. Aoki, T. Harada, K. Ishii, T. Suzuki, S. Nagamori, G. Toda, Y. Matsuura, and T. Miyamura.** 1998. Full-length complementary DNA of hepatitis C virus genome from an infectious blood sample. Hepatology **27:** 621–627.
2. **Aoyagi, K., C. Ohue, K. Iida, T. Kimura, E. Tanaka, K. Kiyosawa, and S. Yagi.** 1999. Development of a simple and highly sensitive enzyme immunoassay for hepatitis C virus core antigen. J. Clin. Microbiol. **37:**1802–1808.
3. **Bartosch, B., J. Dubuisson, and F. L. Cosset.** 2003. Infectious hepatitis C virus pseudo-particles containing functional E1-E2 envelope protein complexes. J. Exp. Med. **197:**633–642.
4. **Bukh, J., R. H. Purcell, and R. H. Miller.** 1993. At least 12 genotypes of hepatitis C virus predicted by sequence analysis of the putative E1 gene of isolates collected worldwide. Proc. Natl. Acad. Sci. USA **90:**8234–8238.
5. **Cerny, A., and F. V. Chisari.** 1999. Pathogenesis of chronic hepatitis C: immunological features of hepatic injury and viral persistence. Hepatology **30:**595–601.
6. **Cocquerel, L., S. Duvet, J. C. Meunier, A. Pillez, R. Cacan, C. Wychowski, and J. Dubuisson.** 1999. The transmembrane domain of hepatitis C virus glycoprotein E1 is a signal for static retention in the endoplasmic reticulum. J. Virol. **73:**2641–2649.
7. **Cocquerel, L., A. Op de Beeck, M. Lambot, J. Roussel, D. Delgrange, A. Pillez, C. Wychowski, F. Penin, and J. Dubuisson.** 2002. Topological changes in the transmembrane domains of hepatitis C virus envelope glycoproteins. EMBO J. **21:**2893–2902.
8. **Dubuisson, J.** 2000. Folding, assembly and subcellular localization of hepatitis C virus glycoproteins. Curr. Top. Microbiol. Immunol. **242:**135–148.
9. **Dubuisson, J., H. H. Hsu, R. C. Cheung, H. B. Greenberg, D. G. Russell, and C. M. Rice.** 1994. Formation and intracellular localization of hepatitis C virus envelope glycoprotein complexes expressed by recombinant vaccinia and Sindbis viruses. J. Virol. **68:**6147–6160.
10. **Dubuisson, J., and C. M. Rice.** 1996. Hepatitis C virus glycoprotein folding: disulfide bond formation and association with calnexin. J. Virol. **70:**778–786.
11. **Grakoui, A., C. Wychowski, C. Lin, S. M. Feinstone, and C. M. Rice.** 1993. Expression and identification of hepatitis C virus polyprotein cleavage products. J. Virol. **67:**1385–1395.
12. **Hijikata, M., N. Kato, Y. Ootsuyama, M. Nakagawa, and K. Shimotohno.** 1991. Gene mapping of the putative structural region of the hepatitis C virus genome by in vitro processing analysis. Proc. Natl. Acad. Sci. USA **88:**5547–5551.
13. **Ho, S. N., H. D. Hunt, R. M. Horton, J. K. Pullen, and L. R. Pease.** 1989. Site-directed mutagenesis by overlap extension using the polymerase chain reaction. Gene **77:**51–59.
14. **Hope, R. G., and J. McLauchlan.** 2000. Sequence motifs required for lipid droplet association and protein stability are unique to the hepatitis C virus core protein. J. Gen. Virol. **81:**1913–1925.
15. **Horton, R. M., H. D. Hunt, S. N. Ho, J. K. Pullen, and L. R. Pease.** 1989. Engineering hybrid genes without the use of restriction enzymes: gene splicing by overlap extension. Gene **77:**61–68.
16. **Hussy, P., H. Langen, J. Mous, and H. Jacobsen.** 1996. Hepatitis C virus core protein: carboxy-terminal boundaries of two processed species suggest cleavage by a signal peptide peptidase. Virology **224:**93–104.
17. **Kail, M., M. Hollinshead, W. Ansorge, R. Pepperkok, R. Frank, G. Griffiths, and D. Vaux.** 1991. The cytoplasmic domain of alphavirus E2 glycoprotein contains a short linear recognition signal required for viral budding. EMBO J. **10:**2343–2351.
18. **Koike, K., and K. Moriya.** 2005. Metabolic aspects of hepatitis C viral infection: steatohepatitis resembling but distinct from NASH. J. Gastroenterol. **40:**329–336.
19. **Krogh, A., B. Larsson, G. von Heijne, and E. L. Sonnhammer.** 2001. Predicting transmembrane protein topology with a hidden Markov model: application to complete genomes. J. Mol. Biol. **305:**567–580.
20. **Kunkel, M., M. Lorinczi, R. Rijnbrand, S. M. Lemon, and S. J. Watowich.** 2001. Self-assembly of nucleocapsid-like particles from recombinant hepatitis C virus core protein. J. Virol. **75:**2119–2129.
21. **Kunkel, M., and S. J. Watowich.** 2004. Biophysical characterization of hepatitis C virus core protein: implications for interactions within the virus and host. FEBS Lett. **557:**174–180.
22. **Lambert, C., and R. Prange.** 2001. Dual topology of the hepatitis B virus large envelope protein: determinants influencing post-translational pre-S translocation. J. Biol. Chem. **276:**22265–22272.
23. **Lindenbach, B. D., M. J. Evans, A. J. Syder, B. Wolk, T. L. Tellinghuisen, C. C. Liu, T. Maruyama, R. O. Hynes, D. R. Burton, J. A. McKeating, and C. M. Rice.** 2005. Complete replication of hepatitis C virus in cell culture. Science **309:**623–626.
24. **Lipp, J., N. Flint, M. T. Haeuptle, and B. Dobberstein.** 1989. Structural requirements for membrane assembly of proteins spanning the membrane several times. J. Cell Biol. **109:**2013–2022.
25. **Lo, S. Y., M. J. Selby, and J. H. Ou.** 1996. Interaction between hepatitis C virus core protein and E1 envelope protein. J. Virol. **70:**5177–5182.
26. **Lopez, S., J. S. Yao, R. J. Kuhn, E. G. Strauss, and J. H. Strauss.** 1994. Nucleocapsid-glycoprotein interactions required for assembly of alphaviruses. J. Virol. **68:**1316–1323.
27. **Ma, H. C., C. H. Ke, T. Y. Hsieh, and S. Y. Lo.** 2002. The first hydrophobic

domain of the hepatitis C virus E1 protein is important for interaction with the capsid protein. J. Gen. Virol. 83:3085–3092.
28. **Matsuo, E., H. Tani, C. K. Lim, Y. Komoda, T. Okamoto, H. Miyamoto, K. Moriishi, S. Yagi, A. H. Patel, T. Miyamura, and Y. Matsuura.** 2006. Characterization of HCV-like particles produced in a human hepatoma cell line by a recombinant baculovirus. Biochem. Biophys. Res. Commun. 340:200–208.
29. **Matsuura, Y., T. Suzuki, R. Suzuki, M. Sato, H. Aizaki, I. Saito, and T. Miyamura.** 1994. Processing of E1 and E2 glycoproteins of hepatitis C virus expressed in mammalian and insect cells. Virology 205:141–150.
30. **Matsuura, Y., H. Tani, K. Suzuki, T. Kimura-Someya, R. Suzuki, H. Aizaki, K. Ishii, K. Moriishi, C. S. Robison, M. A. Whitt, and T. Miyamura.** 2001. Characterization of pseudotype VSV possessing HCV envelope proteins. Virology 286:263–275.
31. **McGinnes, L. W., J. N. Reitter, K. Gravel, and T. G. Morrison.** 2003. Evidence for mixed membrane topology of the Newcastle disease virus fusion protein. J. Virol. 77:1951–1963.
32. **Merola, M., M. Brazzoli, F. Cocchiarella, J. M. Heile, A. Helenius, A. J. Weiner, M. Houghton, and S. Abrignani.** 2001. Folding of hepatitis C virus E1 glycoprotein in a cell-free system. J. Virol. 75:11205–11217.
33. **Meunier, J. C., A. Fournillier, A. Choukhi, A. Cahour, L. Cocquerel, J. Dubuisson, and C. Wychowski.** 1999. Analysis of the glycosylation sites of hepatitis C virus (HCV) glycoprotein E1 and the influence of E1 glycans on the formation of the HCV glycoprotein complex. J. Gen. Virol. 80:887–896.
34. **Michalak, J. P., C. Wychowski, A. Choukhi, J. C. Meunier, S. Ung, C. M. Rice, and J. Dubuisson.** 1997. Characterization of truncated forms of hepatitis C virus glycoproteins. J. Gen. Virol. 78:2299–2306.
35. **Migliaccio, C. T., K. E. Follis, Y. Matsuura, and J. H. Nunberg.** 2004. Evidence for a polytopic form of the E1 envelope glycoprotein of Hepatitis C virus. Virus Res. 105:47–57.
36. **Miller, R. H., and R. H. Purcell.** 1990. Hepatitis C virus shares amino acid sequence similarity with pestiviruses and flaviviruses as well as members of two plant virus supergroups. Proc. Natl. Acad. Sci. USA 87:2057–2061.
37. **Moriishi, K., and Y. Matsuura.** 2003. Mechanisms of hepatitis C virus infection. Antivir. Chem. Chemother. 14:285–297.
38. **Moriishi, K., T. Okabayashi, K. Nakai, K. Moriya, K. Koike, S. Murata, T. Chiba, K. Tanaka, R. Suzuki, T. Suzuki, T. Miyamura, and Y. Matsuura.** 2003. Proteasome activator PA28γ-dependent nuclear retention and degradation of hepatitis C virus core protein. J. Virol. 77:10237–10249.
39. **Moriya, K., H. Fujie, Y. Shintani, H. Yotsuyanagi, T. Tsutsumi, K. Ishibashi, Y. Matsuura, S. Kimura, T. Miyamura, and K. Koike.** 1998. The core protein of hepatitis C virus induces hepatocellular carcinoma in transgenic mice. Nat. Med. 4:1065–1067.
40. **Moriya, K., K. Nakagawa, T. Santa, Y. Shintani, H. Fujie, H. Miyoshi, T. Tsutsumi, T. Miyazawa, K. Ishibashi, T. Horie, K. Imai, T. Todoroki, S. Kimura, and K. Koike.** 2001. Oxidative stress in the absence of inflammation in a mouse model for hepatitis C virus-associated hepatocarcinogenesis. Cancer Res. 61:4365–4370.
41. **Mottola, G., N. Jourdan, G. Castaldo, N. Malagolini, A. Lahm, F. Serafini-Cessi, G. Migliaccio, and S. Bonatti.** 2000. A new determinant of endoplasmic reticulum localization is contained in the juxtamembrane region of the ectodomain of hepatitis C virus glycoprotein E1. J. Biol. Chem. 275:24070–24079.
42. **Niwa, H., K. Yamamura, and J. Miyazaki.** 1991. Efficient selection for high-expression transfectants with a novel eukaryotic vector. Gene 108:193–199.
43. **Ogino, T., H. Fukuda, S. Imajoh-Ohmi, M. Kohara, and A. Nomoto.** 2004. Membrane binding properties and terminal residues of the mature hepatitis C virus capsid protein in insect cells. J. Virol. 78:11766–11777.
44. **Okamoto, K., K. Moriishi, T. Miyamura, and Y. Matsuura.** 2004. Intramembrane proteolysis and endoplasmic reticulum retention of hepatitis C virus core protein. J. Virol. 78:6370–6380.
45. **Pavio, N., D. R. Taylor, and M. M. Lai.** 2002. Detection of a novel unglycosylated form of hepatitis C virus E2 envelope protein that is located in the cytosol and interacts with PKR. J. Virol. 76:1265–1272.
46. **Ralston, R., K. Thudium, K. Berger, C. Kuo, B. Gervase, J. Hall, M. Selby, G. Kuo, M. Houghton, and Q. L. Choo.** 1993. Characterization of hepatitis C virus envelope glycoprotein complexes expressed by recombinant vaccinia viruses. J. Virol. 67:6753–6761.
47. **Shimoike, T., S. Mimori, H. Tani, Y. Matsuura, and T. Miyamura.** 1999. Interaction of hepatitis C virus core protein with viral sense RNA and suppression of its translation. J. Virol. 73:9718–9725.
48. **Shintani, Y., H. Fujie, H. Miyoshi, T. Tsutsumi, K. Tsukamoto, S. Kimura, K. Moriya, and K. Koike.** 2004. Hepatitis C virus infection and diabetes: direct involvement of the virus in the development of insulin resistance. Gastroenterology 126:840–848.
49. **Vaux, D. J., A. Helenius, and I. Mellman.** 1988. Spike-nucleocapsid interaction in Semliki Forest virus reconstructed using network antibodies. Nature 336:36–42.
50. **Wakita, T., T. Pietschmann, T. Kato, T. Date, M. Miyamoto, Z. Zhao, K. Murthy, A. Habermann, H. G. Krausslich, M. Mizokami, R. Bartenschlager, and T. J. Liang.** 2005. Production of infectious hepatitis C virus in tissue culture from a cloned viral genome. Nat. Med. 11:791–796.
51. **Zhong, J., P. Gastaminza, G. Cheng, S. Kapadia, T. Kato, D. R. Burton, S. F. Wieland, S. L. Uprichard, T. Wakita, and F. V. Chisari.** 2005. Robust hepatitis C virus infection in vitro. Proc. Natl. Acad. Sci. USA 102:9294–9299.